

University of Reading
School of Mathematics, Meteorology & Physics

Anomalous Diffusion
by

Lee Morgan

August 2007

This dissertation is submitted to the Department of Mathematics in partial fulfilment
of the requirements for the degree of Master of Science

Contents

ABSTRACT	2
GLOSSARY	3
1 INTRODUCTION.....	4
1.1 FRACTIONAL DIFFUSION EQUATION.....	6
1.2 EXAMPLES OF ANOMALOUS TRANSPORT	8
1.3 THEORETICAL APPLICATIONS OF FRACTIONAL DERIVATIVES	10
1.4 UNDERLYING PHYSICS OF SUPERDIFFUSION.....	11
1.5 RANDOM WALKS AND LEVY FLIGHTS.....	14
1.6 PROBABILITY DISTRIBUTIONS	15
1.7 2D LEVY WALK	17
1.8 LEVY FLIGHTS.....	17
1.9 THEORY OF FRACTIONAL CALCULUS	18
2 1D FRACTIONAL DIFFUSION.....	21
2.1 A NUMERICAL APPROXIMATION FOR THE 1D FRACTIONAL DIFFUSION EQUATION	21
2.2 A 1D NUMERICAL EXAMPLE.....	23
2.3 QUALITATIVE BEHAVIOR OF FRACTIONAL DIFFUSIVE SYSTEMS	25
2.4 FULL WIDTH AT HALF MAXIMUM.....	27
2.5 MEAN SQUARE DEVIATION	28
2.6 ITERATION MATRICES	31
2.7 FRACTIONAL FOKKER-PLANK EQUATION	34
3 2D FRACTIONAL DIFFUSION.....	37
3.1 A NUMERICAL APPROXIMATION FOR THE 2D FRACTIONAL DIFFUSION EQUATION	37
3.2 A 2D NUMERICAL EXAMPLE.....	39
3.3 2D DIFFUSION.....	41
3.4 SKEWED DIFFUSION	43
4 2D PLUME DIFFUSION	44
5 FUNCTIONAL ORDER DERIVATIVES.....	46
5.1 AN EXTENSION OF FRACTIONAL DERIVATIVES	46
6 SUMMARY	51
REFERENCES	54

Abstract

Fractional dynamics is a well documented subject, which has applications in a very diverse range of areas. Some of the aims of the report are to produce a brief overview of the theory and applications of fractional dynamics, create a physical picture of what is causing fractional dynamics and explain the link between fractional diffusion and Levy dynamics. The core of the report focuses on the fractional diffusion equation in 1 and 2 dimensions whereby a description of sub-diffusion and super-diffusion is described, aided by computed simulations. Reproductions of results from significant papers in the subject of fractional diffusion are also produced. The phenomenon of anomalous plume diffusion is also simulated using the 2D fractional advection-diffusion equation. In the later part of the report the derivation, description and examples of functional order fractional diffusion is presented, which as far as the author is concerned is original.

Glossary

Brownian Motion : The random movement of particles whose probability density function is a Gaussian distribution.

Diffusion : The phenomena of random movements causing an imbalance of some system to change until the system is in equilibrium.

Anomalous Diffusion : A form of diffusion whereby the rate at which the system equilibrium is reached is unlike that of standard diffusion.

Random Walk : A random motion that assigns each jump with a length x which occurs at regular intervals. The size of the jump x is specified by a probability distribution.

Levy Flight : A particular type of random walk whereby the the waiting times between jumps if dependant on the size of the jump. The probability density function is long tailed when compared to the Gaussian.

Langevin Equations : A stochastic differential equation that describes the random movements of particles using Newtonian physics with an addition fluctuation.

Advection : The transport of a scalar quantity by a vector field.

Probability Density Function(PDF) : A function that describes the probability of finding a particles in a particular position in space.

1 Introduction

All students/researchers whose subject area falls under the umbrella of mathematical physics will have at some point either implemented and/or studied the standard diffusion equation(1).

$$\frac{\partial U(r,t)}{\partial t} = \nabla^2 U(r,t) + S(r,t) \quad (1)$$

Where U is the density of the diffusing material and S is a forcing term (sometimes called a sink/source).

Superdiffusion is a form of anomalous diffusion that occurs faster than the standard diffusion equation (1) would predict. A more generalized diffusion equation that encompasses superdiffusion (and its antonym, subdiffusion) is called the fractional diffusion equation. There are two types of fractional diffusion equation. The first(2) has a fractional derivative in the spatial part[1] and the second(3) has a fractional derivative in time[10].

$$\frac{\partial U(r,t)}{\partial t} = \nabla^\alpha U(r,t) + S(r,t) \quad (2)$$

$$\frac{\partial^\beta U(r,t)}{\partial t^\beta} = \nabla^2 U(r,t) + S(r,t) \quad (3)$$

The fractional equation stems from subject area of fractional calculus. Differential and integral operators within fractional calculus are not confined to integer orders (d/dx , d^2/dx^2 , d^3/dx^3 etc) and can be of fractional orders (i.e. $d^{0.7}/dx^{0.7}$, $d^{2.6}/dx^{2.6}$, d^{-1}/dx^{-1} etc). The difference between the spatially fractional diffusion equation and the standard equation is the exponent of the Laplacian operator is no longer 2 and can in fact be any real number.

The standard method of measuring the spread of time fractional diffusion is the mean square deviation (MSD). The evolution of the distribution of the diffusive material can be defined using a simple MSD equation

$$\langle \delta x^2(t) \rangle = Mt^\theta \quad (4)$$

where $\delta x(t) = x(t) - \langle x(t) \rangle$. The value of the exponent, theta, determines the class of diffusion of the system.

The derivative exponent in the time fractional diffusion equation has the relation

$$\theta = 3 - \beta \quad 1 \leq \beta \leq 2 \quad (5)$$

The MSD cannot be expressed in a simple equation for spatially fractional diffusion. Instead, the diffusion is measured more proficiently by the Full Width at Half Maximum(FWHM).

$$FWHM \propto t^\theta \tag{6}$$

Where $\theta = \alpha/2$ (proof provided in section 2.4)

Diffusion exponent	Diffusion class
$\theta = 1$	No diffusion(advection)
$1 < \theta \leq 2$	Sub-diffusion
$\theta = 2$	Normal diffusion

Table 1 – Classification of diffusion by exponent

One point that may be slightly ambiguous if not addressed is that the anomalous diffusion that needs to be described using the fractional equation is not caused by the breakdown of classical diffusion. Instead, it is caused by external effects which either have been purposely neglected due to either lack of knowledge of the system or because there are far too many variables to compute. For example, the anomalous diffusion of plasmas is caused by neglecting Maxwell's equations and quantum mechanics in the simulation, the anomalous flow of water in the water table is due to geological structure and complex macroscopic behavior being neglected. The anomalous transport of monkeys(Metzler et al.) is not anomalous at all because it is ludicrous that such a simple equation such as equation 3 could describe the movement of such an incredibly complicated system that is a monkey.

Anomalous diffusion is closely linked with transport theories. The simulation of fluids or plasmas can be approached from many different levels, which include

- A totally mechanical theory that encompasses Newton's laws of motion, relativistic mechanics, Maxwell's equations, Navier-Stokes equation etc. This method has the potential to be most accurate and reliable, however implementing this is incredibly computationally expensive and in many cases the required resolution cannot be achieved without some simplifications or assumptions.
- A stochastic-mechanical description that combines Newton's laws with an added fluctuating field. Examples of this are V-Langevin equations. A short description of on method is given in section 1.4.
- Fractional diffusion and continuous time random walks (CTRW) are semi-mechanical in the way that they commonly use transport equations, and semi-stochastic in the way that they use statistical theories to create CTRW's but on the other hand they are neither mechanical nor statistical due to the fact that the equations that describe the anomalous transport use empirical fitting and cannot be derived deterministically. This is the approach that will be focused upon for the rest of the report.

1.1 Fractional Diffusion Equation

The standard diffusion equation is a partial differential equation that describes the density of a diffusing material as a function of space and time. It has a relatively simple derivation that merges the continuity equation(7) with Fick's Law(8). If $U(x,t)$ is the density of the diffusing material at any point in time and space and $\bar{\mathbf{j}}$ is the flux of the diffusive material entering an infinitesimal volume at the position $(\underline{\mathbf{x}},t)$ then the following equations apply.

$$\frac{\partial U}{\partial t} + \nabla \cdot \bar{\mathbf{j}} = 0 \quad (7)$$

$$\bar{\mathbf{j}} = -D \nabla U \quad (\text{Flux is proportional to concentration gradient}) \quad (8)$$

Where D , the diffusivity, is associated with the Einstein-Stokes equation(9)

$$D = \frac{k_B T}{6\pi\eta r} = \mu k_B T \quad (9)$$

k_B is Boltzmann's constant, T is temperature, η is friction/viscosity coefficient, μ is mobility and r is the radius of a spherical particle.

When Fick's Law (8) is substituted into the continuity equation(7) the standard diffusion(with no forcing term) equation emerges.

$$\frac{\partial U}{\partial t} + \nabla \cdot (-D \nabla U) = 0$$

$$\therefore \frac{\partial U}{\partial t} = D \nabla^2 U$$

If an outside force is applied which has the effect of altering the natural diffusion then an additional flux term is included in Fick's Law. When Fick's law is substituted into the continuity equation the gradient of the additional flux terms appears which is normally stated as simple function.

$$\frac{\partial U}{\partial t} = D \nabla^2 U + \nabla q = D \nabla^2 U + S \quad (10)$$

The standard diffusion equation(10) ,with no forcing term, governs Brownian motion and generates an exponent equal to unity in equation 4&6 and results in the MSD being linearly proportional to time (proof provided in section 2.5).

$$\langle \delta x^2(t) \rangle = Mt \quad (11)$$

Aside: An interesting fact is that equation 11 was first published in 1905[20] by Albert Einstein in the third of his seminal papers which he published while doing his PhD in statistical mechanics (The first and second were based on the photoelectric effect and special relativity respectively). It is this paper on statistical mechanics which is Einstein's most cited article despite the fact that he received the Nobel Prize for his work on the photoelectric effect and he is best known for his work in relativity. This paper helped cement the idea that atoms/molecules existed and along with his other papers became the foundations of quantum mechanics.

The probability density function $U(x,t)$ describing the probability, $U(x,t)dx$, of finding of finding a particle between x and $x+dx$ given an initial condition $U(x,0)=\delta(x)$ the solution becomes the well known Gaussian[12](proof provided in section 2.4).

$$U(x,t) = (4\pi Dt)^{1/2} \exp(-x^2 / 4Dt) \quad (12)$$

The fractional diffusion equation arises from the fractional form of Fick's Law, although, arguably it could stem from a hypothetical fractional continuity equation. A fractional form of Fick's Law is more physically plausible than a fractional continuity equation as Fick's law is more empirical in nature.

$$j = -D_\beta \nabla^\beta U + S \quad (13)$$

$$\frac{\partial U}{\partial t} = D_\beta \nabla^{1+\beta} U + \nabla q = D_\alpha \nabla^\alpha U + S \quad (14)$$

The governing dynamics that control the diffusion is non-Brownian in nature and produces a probability density function(12)[5] that is quasi-Gaussian that has heavier tails than the standard Gaussian(for $S=0$).

$$U(x,t) = (4\pi D_\alpha t^\alpha)^{1/2} \exp(-x^2 / 4D_\alpha t^\alpha) \quad (15)$$

Note that the diffusivity, D , now has a subscript to imply that the value of D_α for the fractional diffusion equation is dependant on the value of alpha. This is due to dimensionality of the fractional derivative. The SI units of D is m^2s^{-1} , whereas the SI units for D_α is $m^\alpha s^{-1}$.

1.2 Examples of Anomalous Transport

There is an enormous amount of papers published on the subject so called anomalous transport and anomalous diffusion. The word anomalous is slightly ambiguous as it suggests that the processes/events taking place are not understood, yet in almost all scenarios the process is well understood. The word anomalous refers to the non-Gaussian nature of the governing statistics and can be explained using Levy statistics. The following pages describe a number of scenarios where Levy statistics are present and they may be labeled with the terms anomalous transport or anomalous diffusion.

DNA – In the coding and non-coding of nucleotide sequences long range correlations have been found that obey Levy distributions [6,7]. A nucleotide (aka base. A rung of the helical ladder) is a chemical compound that consists of 3 portions: a heterocyclic base, a sugar, and one or more phosphate groups[5]. A method presented in ref [7] describes an artificial sequencing technique that shows that power law correlations are present in both coding and non-coding sequences. i.e. DNA bases that code proteins are not only correlated to their neighbouring bases but also have long range correlations with other bases. Figure 4 shows that the entropy follows a power law similar to that of equation 3.

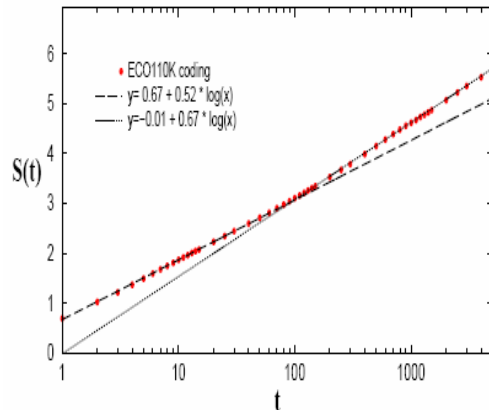


Fig 4 - The diffusion entropy analysis for a DNA sequence result in a scaling changing with time.

Microbiology [24] – The transport behavior of microspheres within cells have been found to have superdiffusive behavior with an exponent $\alpha = 3/2$ when applied to eqn 3. This superdiffusive behavior is often followed by either normal diffusion or subdiffusion. The exponent of $3/2$ generates suspicion as this is very close to the exponent of a random velocity field. Note that the MSD starts to plateau at long times. This is likely to be caused by boundary effects that cause the microspheres move back towards the origin.

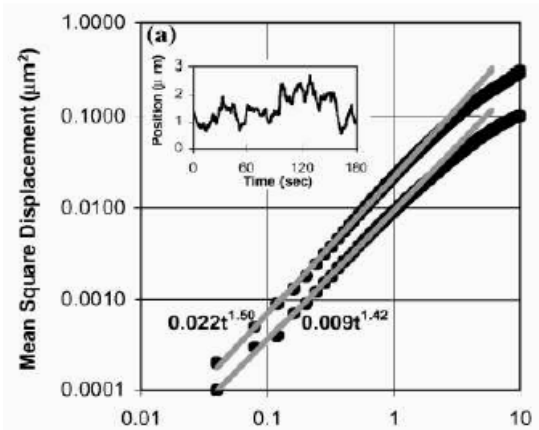


Fig 5 – The mean square displacement of microspheres w.r.t time showing fractal behavior

Paleomagnetism – Local measurements of the geomagnetic field show that the polarity of the geomagnetic field has occasionally flipped. The earth’s magnetic field is generated by electric currents in the liquid outer core. The movement of the electric current is complex and is governed by the same magnetohydrodynamic theory of nuclear plasma physics. The pole is not stationary and in fact it roams up to 40km per year[39] around the cartographical North Pole. Occasionally, the north-south dipoles rotate 180 degrees and what was the North Pole is now the South Pole and visa-versa. The persistence times of the meta-stable states of geomagnetic dynamo have been found to obey Levy statistics [8].

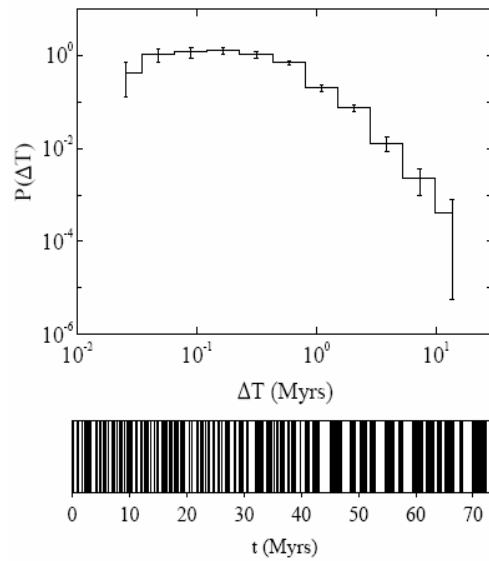


Fig 6 – Upper: probability density function of persistence times. Lower: Polarity of the earth's magnetic field (Solid bar = present)

Astrophysics[25] – The anomalous scaling relations of signals being received from pulsars have recently been made clear due the theory that electron density fluctuations in the interstellar medium obey Levy statistics. Previous analyses of interstellar scintillations of signals were believed to be of a Gaussian nature. Theory that explains the previously anomalous behavior suggests that the probability distribution of density gradients has power-law decay. It suggests that the ray angle performs a Levy flight and not a random walk as previously assumed.

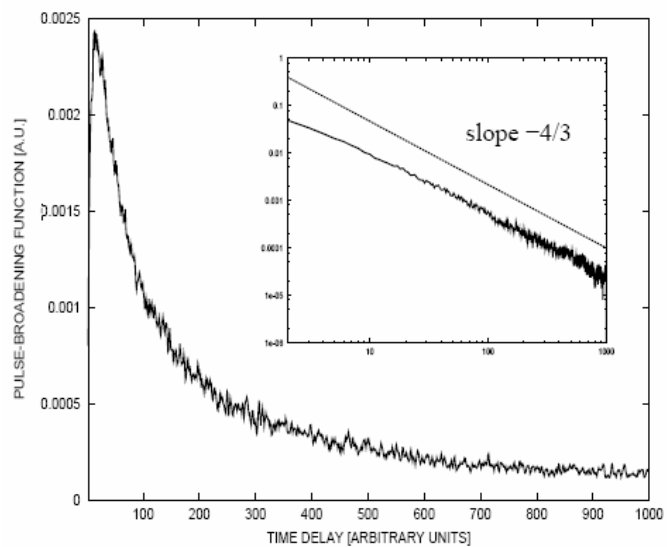


Fig 7 – The fractal behavior of Electromagnetic signal angle distribution.

Quantum Dots[26] - Arrays of semiconductor nanocrystals (quantum dot arrays, or QDAs) can be designed in order to control the Hamiltonian and therefore create materials with desirable transport properties. The transport properties of QDA's are not well understood and several theories exist that explain anomalous electron transport. One theory that explains a recently observed transient power-law decay(15) of current uses Levy statistics applied to waiting on/off times to describe the behaviour of the current(I) as a response to large bias voltage being applied across the array.

$$I(t) = I_0 t^{-\alpha} \quad 0 < \alpha < 1$$

1.3 Theoretical Applications of Fractional Derivatives

Fractional Schrödinger Equation[28] – The Schrödinger equation is a quantum mechanical equation that uses the wave picture (and notably the first to do so) to describe the behavior of matter at very small scales. The fractional equation has predicted the energy levels of a hypothetical fractional Bohr atom.

Fractional Telegraph Equations[29,30] – These equations can be thought of as a simplified version of Maxwell's equations are used to describe the current and voltage behavior in a lossy wire. The fractional derivative compliments the standard equation by incorporating anomalous wave and diffusive behavior into the model.

Fractal Hydrodynamic Equations [31] – These equations are often used to describe the hydrodynamic behavior in porous media. The pore space in real media is extremely complex and irregular geometry and as such their contribution to hydrodynamic flow doesn't fit standard Euclidian hydrodynamics equations. A set of fractional Euler and Navier-Stokes equations can match the fractal geometry of the porous media, hence, it can successfully model complex hydrodynamic behavior.

The fractional Fokker-Planck equation is a well studied fractional equation which will be discussed in more detail later in the report(section 2.10).

1.4 Underlying Physics of Superdiffusion

One of the underlying principles in which the derivation of the standard diffusion equation is based upon is that the medium the diffusive material is traveling in is isotropic and homogeneous and that the diffusive material is stationary. The conditions under which anomalous diffusion occurs do not match the underlying principles of the diffusion equation derivation and so there is no surprise that the standard equation will not accurately describe anomalous diffusive behavior.

Physical entities that cause superdiffusion include energy potentials such as electric fields, magnetic fields, gravitational fields etc. These potentials cause the diffusive particles to get trapped in potential wells and when the trapped particles have energies below that of the potential barrier then it will be trapped until either it can either gain enough energy to escape or until the potential well has decayed/changed. The large spatial jump that characterizes Levy walks and anomalous diffusion can be caused by the rapidly changing potentials combined with trapped particles gaining momentum while in the force field. The particle gets trapped and is pulled towards the potential minimum and while it is traveling it gains kinetic energy from the work done by the field on the particle. When it is near the potential minimum it will have a high kinetic energy. Now, if the field was to rapidly change the particle will have excess kinetic energy and when it tries to escape it will overshoot and will travel a large distance. This can be easily visualized with a seed floating in a moving bucket of water (fig. 1).

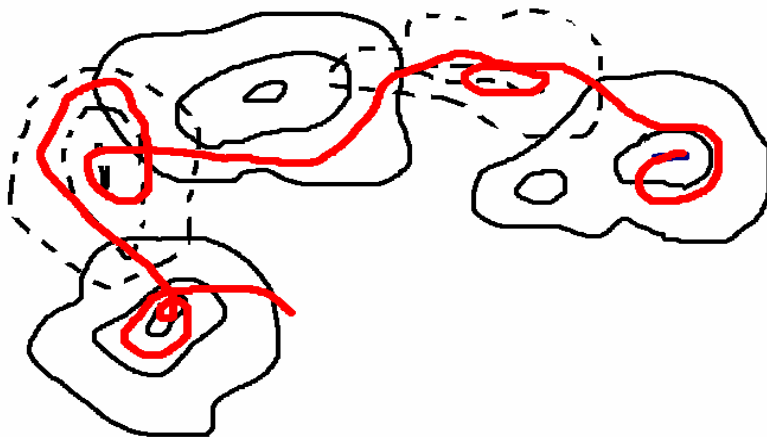


Fig 1 – A visualization of a seed traveling in turbulent water. The seed travels locally within vorticity potentials until the potential changes and then the seed undergoes a sling shot action and travels a large distance until it next gets trapped in a vorticity potential.

The principle of particles moving along contour lines or potential wells is some times referred to as particle “roads”[3]. The roads lead the particles in particular directions and influence their speed while on these roads. Classical Brownian motion, which leads to the description of classical diffusion has no roads and has a Gaussian spatial correlation function. The motion illustrated in fig 1, which can be described with fractional diffusion provides roads for the

particles to travel along. This movement, known as a Levy walk, leads to a non-Gaussian spatial correlation function that is described by Levy statistics.

The phenomena of Levy walks is demonstrated in Lacasta et al.[4] where Langevin equations are implemented in order to simulate the movement/diffusion of particles in periodic and random potentials. The model is based on the equations of motion

$$\begin{aligned} m\ddot{x} &= -\frac{\partial}{\partial x}V\left(\frac{x}{\lambda}, \frac{y}{\lambda}\right) - \mu\dot{x} + \xi_x(t) \\ m\ddot{y} &= -\frac{\partial}{\partial y}V\left(\frac{x}{\lambda}, \frac{y}{\lambda}\right) - \mu\dot{y} + \xi_y(t) \end{aligned} \tag{16}$$

Where m is the mass, V is potential, μ is the coefficient of friction, λ is a scaling coefficient and ξ is white noise.

The simulation involves releasing an ensemble of thousands of particles within a specified potential and moving these particles using the Langevin equations (16) that replicate the processes involved in thermal fluctuations. The position of the particles and the collective mean square deviation is recorded at every time step. The development of the MSD is highly dependant on the potential, the friction coefficient and also the initial velocity distribution of the particles.

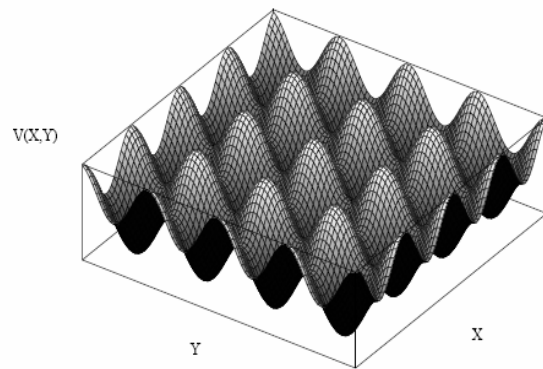


FIG 2 [4] – A finite portion of the much larger two dimensional periodic potential in which a particles diffuse.

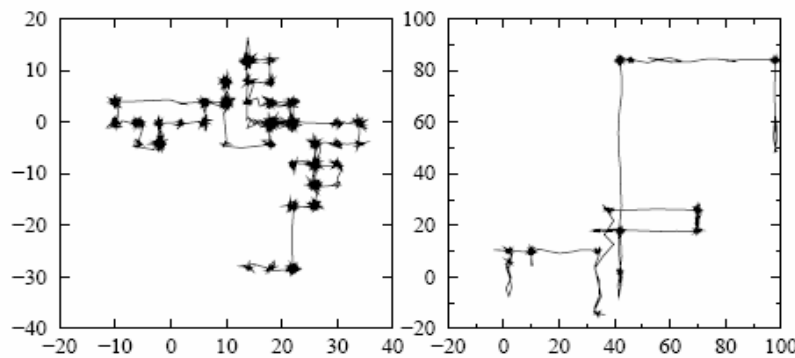


FIG 3 [4] – Left: A trajectory for $\mu=1$ over 20,000 time units. Right: A trajectory for $\mu=0.04$ over 15,000 time units

Figure 3 shows the effect that the friction has on the transport of the particles within the potential. As expected, the movement of particles which are acted upon by relatively high friction have significantly reduced freedom. This is due to the particles having to overcome

the forces from potential wells and friction and so they become trapped in the cells more often than in the case where is friction is present. This is evident from the larger globules found in potential wells in figure 3. Figures 4 & 5 show that the initial velocity distribution of particles affects the movement on the short time scale but eventually the particles are all slowed down to roughly the same speed and at very long times the memory of the initial conditions is lost.

The diffusion is clearly of a fractional nature at small times, and gradually converges towards standard diffusion. Note that the change in gradient is caused by a change(decay) of a driving force in the system whereby another driving force takes preference over the last. This topic will be discussed and resolved later in the section named Functional Order Derivatives.

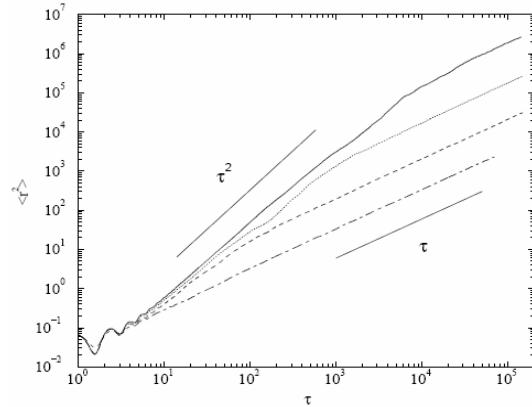


FIG 4 – [4] Mean square displacement vs. time for an ensemble of 5000 particles in the periodic potential with a Maxwell-Boltzmann initial velocity distribution for a range of friction coefficients. (solid=0.0004, dotted = 0.004, dashed=0.04 and dot-dash=0.4)

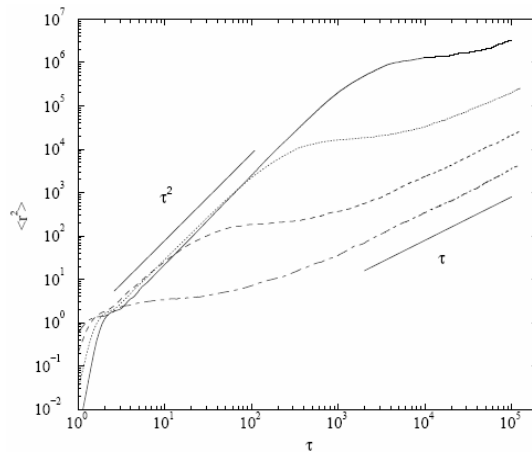


FIG 5 – [4] Mean square displacement vs. time for an ensemble of 5000 particles in the periodic potential with zero velocity for a range of friction coefficients.

1.5 Random Walks and Levy Flights

A continuous time random walk describes the random motion of a particle that jumps a specified distance x , determined by a probability density $\lambda(x)$, at time intervals determined by $\psi(t)$. The standard Brownian motion is created by a Gaussian probability density. The most basic random walks have constant jump length, each jump is performed at regular intervals and there is no preferred direction for each jump, hence the process is Markovian. The applications of random walks are plentiful and to name just a few:

- Economics- Modeling share prices [10,17,18]
- Linguistics – Modeling the distribution of languages[11]
- Human movement – Several versions of this theory exist which range from the modeling of escaped prisoners during war times to the modeling of what pub a drunk sailor is most likely to be found.
- The first random walk was recognized by Robert Brown, a botanist. He noticed that grains of pollen and dust were randomly moving in water with no correlation. (Another claim to fame of his was that he named the cell nucleus[19,21]).

Levy Flights(LF) are a special type of random walk whereby the probability density $\lambda(x)$ is characterized by broader tails than the Gaussian (as associated with standard random walk) that allows a broader jump length distribution. This causes the mean square displacement of a levy flight to diverge.

$$P(x,t) = \mathfrak{F}^{-1} \left\{ \exp\left(-K^\alpha t |x|^\alpha\right) \right\} \approx K^\alpha t / |x|^{\alpha+1} \quad 0 < \alpha \leq 2$$

Random walks are equivalent to standard diffusion and LF's are equivalent to fractional diffusion.

A particular type of LF that possesses a finite mean square displacement is a Levy walk. The finite MSD is formed by coupling the time and spatial probability distributions such that long jumps are penalized by long waiting times.

$$P(k,u) = \frac{1}{u} \psi(u) / [1 - \psi(k,u)] \quad \therefore \psi(t) \approx \tau^\alpha / t^{1+\alpha}$$

$$\psi(x,t) = \frac{1}{2} |x|^{-\mu} \delta(|x| - \nu_v t^\nu) \quad \nu u > 1$$

1.6 Probability Distributions

The probability of finding a particle in the region x to $x+dx$ in the Brownian diffusion scheme, given a Delta wave initial condition, always has a Gaussian density distribution. However, in the fractional case the probability density function is a Levy distribution. The Levy distribution is characterized by the broader tails when compared to the Gaussian distribution.

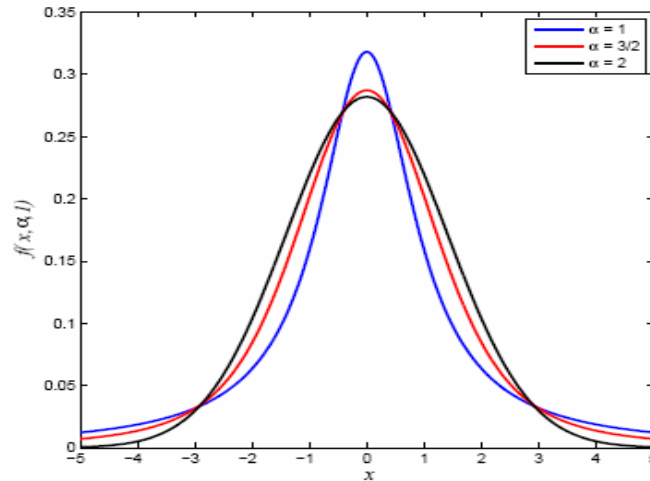


Fig 6 – Symmetric stable distributions with $\alpha = 1, 1.5$ and 2 .

Figure 7 shows four 1D random walks of 1000 steps whose step length is dependant on the Levy distribution. The Levy distributions with $\alpha=1$ and $\alpha =2$ are the well known Cauchy and Gaussian distributions.

The figures clearly show that the Levy walks with low α values are characterized by large jumps due to the thicker tails of the distribution that increase the probability of producing large values. Observe the difference in scales on the three graphs. The lower α values significantly increase the range of position values.

Comparing fig 8 with fig 1 makes the link between turbulent/anomalous transport with Levy distributions. Figure 1 shows an idealized map of the movement of a particle in turbulent medium that causes many small steps along with some sporadic large jumps. The random walk can be thought of as a particles trying to search(or travel to) every part of the domain. The Levy walk with low alpha value will visit every part of the domain in a far quicker time than a levy Walk with a high alpha, albeit a very fleeting visit for the low alpha particle in many cases.

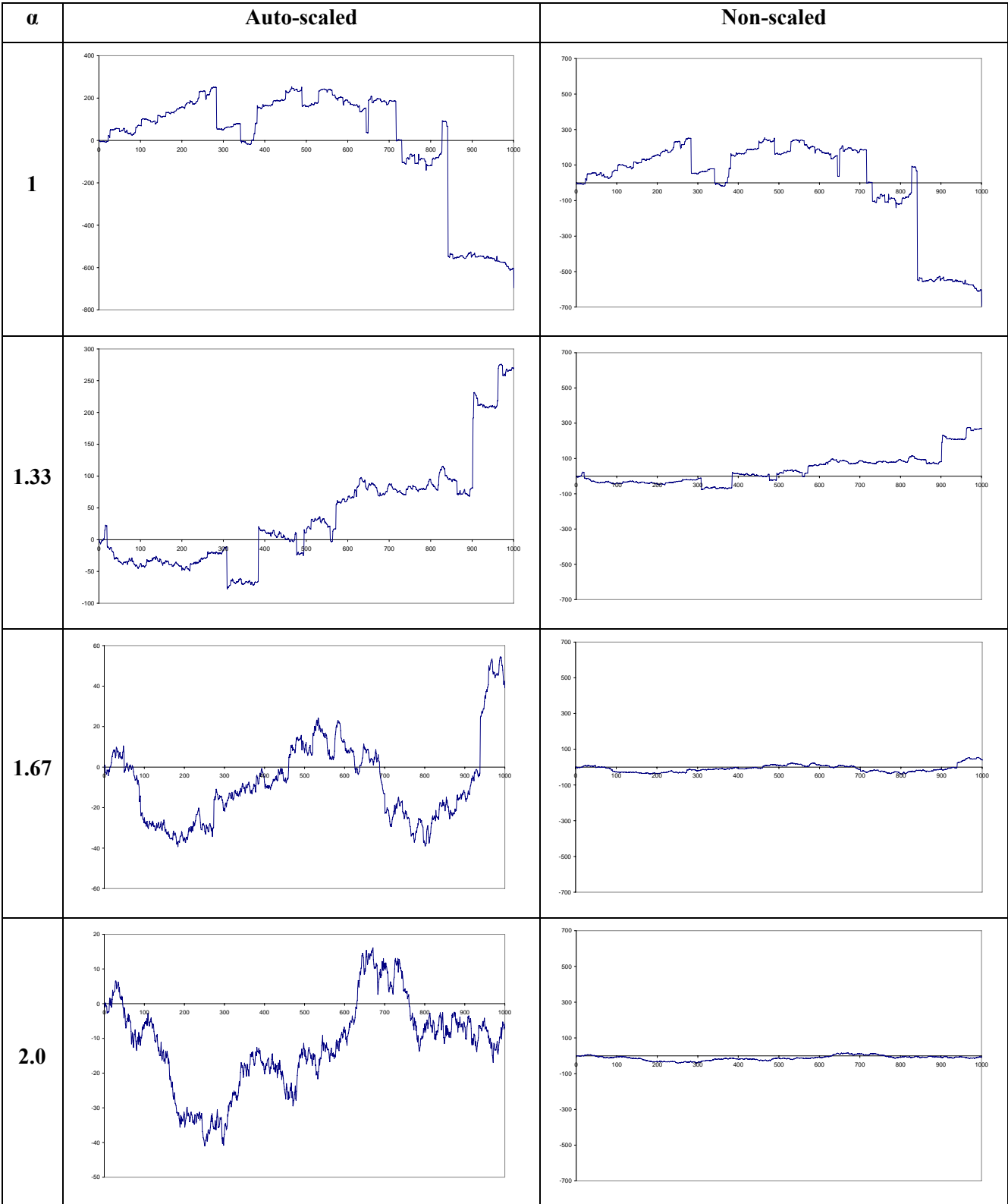


Fig 7 – Scaled and non-scaled 1D levy random walk for $\alpha = 1, 1.33, 1.67$ and 2.0 .

1.7 2D Levy Walk

The purpose of this next section is to use 2D Levy walks to create a model solution to compare with the fractional diffusion equation. One thousand particles will be released and at set intervals their mean square deviation and average displacement will be calculated. These results can then be compared to both the analytic solutions and solutions of the fractional diffusion equation.

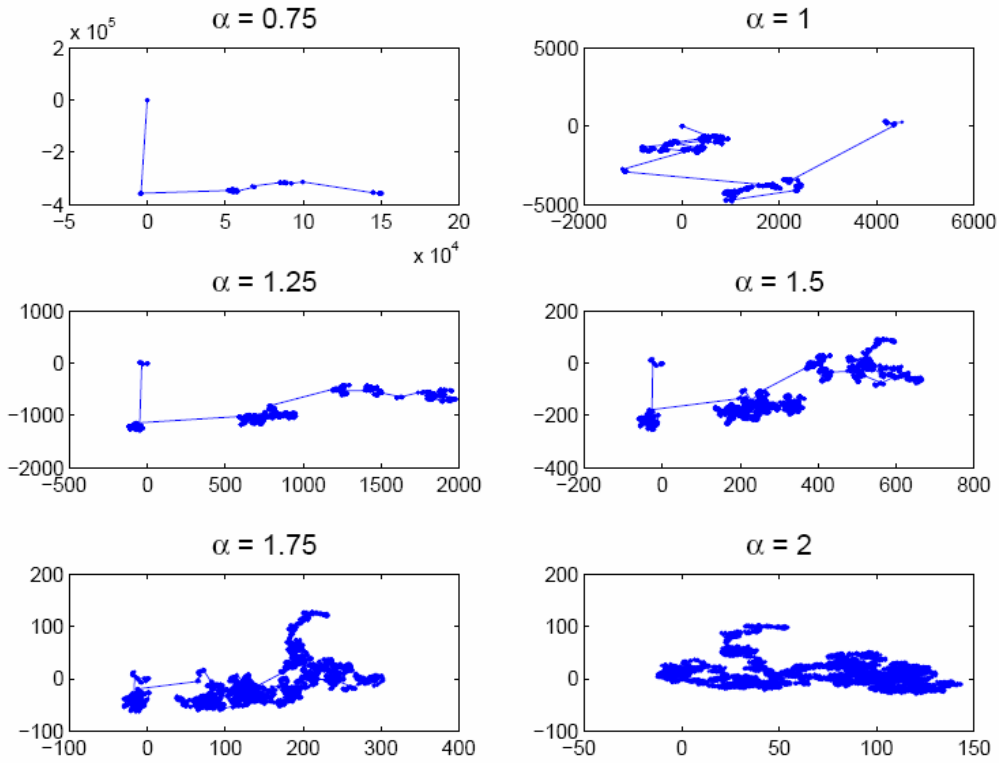


Fig 8[27] – Levy Walk for various values of α . The Levy distribution used here is symmetric. i.e. $\beta=0$.

1.8 Levy Flights

The linear time dependence of the MSD characterizes standard diffusion. To produce non linear time dependence, i.e. anomalous diffusion, Levy flights must be used. Levy flights are similar in nature to Levy walks except that movements are not equally spaced in time. Producing a levy flight using computer code is difficult, but an approximated Levy flight is relatively simple using eqn (17). Allowing the random walker to make steps of length l distributed as[15]

$$P(\ell) = \frac{C}{(1 + \ell)^{1+\beta}} \quad (17)$$

Where C is a normalization constant, the MSD can be shown to behave

in the following manner [15]

$$\langle \delta x^2(t) \rangle \approx \begin{cases} t^2 & 0 < \alpha < 1 \\ t^2 / \ln \ell & \alpha = 1 \\ t^{3-\beta} & 1 < \alpha < 2 \\ t \ln t & \alpha = 2 \\ t & \alpha > 2 \end{cases} \quad (18)$$

1.9 Theory of Fractional Calculus

The concept of fractional calculus is nearly as old as the concept as calculus itself. Leibniz mentioned the concepts of fractional calculus in a letter to L'Hospital in 1695[2]. Later, more comprehensive studies of the concept were made by Euler(1730), Lagrange(1772), Liouville(1832), Holmgren(1864), Riesz(1949), Riemann (1953). Duff(1956), Courant and Hilbert(1962)[2]. There are almost as many definitions of a fractional derivative as there are mathematicians that studied them, but only two definitions(and their derivations) will be shown here. The first (i) definition is in terms of nth order integrals and the second (ii) in terms of limits of difference quotients.

(i) The standard notation of an n^{th} derivative of a function F with respect to x for a positive integer is[14]

$$\frac{d^n f}{dx^n}$$

Due to integration and differentiation being inverse operations it is logical to assume that a differential operator with negative exponent implies integration.

$$\frac{d^{-1} f}{[dx]^{-1}} \equiv \int_0^x f(y) dy$$

Differential operators are additive in nature and so the following can be deduced

$$\frac{d^{-2} f}{[dx]^{-2}} \equiv \int_0^x dx_1 \int_0^{x_1} f(x_0) dx_0$$

$$\frac{d^{-n} f}{[dx]^{-n}} \equiv \int_0^x dx_{n-1} \int_0^{x_{n-1}} dx_{n-2} \cdots \int_0^{x_2} dx_1 \int_0^{x_1} f(x_0) dx_0$$

Another identity of integral operators is called upon in order to enable the lower limit of the integral to be non-zero.

$$\int_a^x f(y) dy \equiv \int_0^{x-a} f(y+a) dy$$

Thus, the following can be defined:

$$\frac{d^{-1}f}{[d(x-a)]^{-1}} \equiv \int_a^x f(y)dy$$

Again, using the additive property of differential operators gives:

$$\frac{d^{-n}f}{[d(x-a)]^{-n}} \equiv \int_a^x dx_{n-1} \int_a^{x_{n-1}} dx_{n-2} \cdots \int_a^{x_2} dx_1 \int_a^{x_1} f(x_0)dx_0$$

(ii) The second definition stems from backward differencing scheme[15]

$$\frac{d^1f}{dx^1} \equiv \lim_{\Delta x \rightarrow 0} \left\{ \frac{f(x) - f(x - \Delta x)}{\Delta x} \right\}$$

The second derivative is

$$\frac{d^2f}{dx^2} \equiv \lim_{\Delta x \rightarrow 0} \left\{ \frac{f(x) - 2f(x - \Delta x) + f(x - 2\Delta x)}{[\Delta x]^2} \right\}$$

And the nth derivative can be deduced using the observation that the coefficients are binomial coefficients of alternating sign. Hence

$$\frac{d^n f}{dx^n} \equiv \lim_{\Delta x \rightarrow 0} \left\{ [\Delta x]^{-n} \sum_{j=0}^n [-1]^j \binom{n}{j} f(x - j\Delta x) \right\}$$

In order to define the derivative in terms of a restricted limit and restrict the derivative to discrete values only, a redefinition of dx is needed. The redefinition that allows this is

$$\Delta x = \frac{x - a}{N}$$

Where N = 1,2,3... and a < x and is similar to a lower limit in an integral sense. The nth derivative can now be written as

$$\frac{d^n f}{dx^n} \equiv \lim_{\Delta x \rightarrow 0} \left\{ \frac{\sum_{j=0}^{N-1} [-1]^j \binom{n}{j} f(x - j\Delta x)}{[\Delta x]^n} \right\} = \lim_{N \rightarrow \infty} \left\{ \frac{\sum_{j=0}^{N-1} [-1]^j \binom{n}{j} f\left(x - j \left[\frac{x-a}{N} \right]\right)}{\left[\frac{x-a}{N} \right]^n} \right\}$$

The binomial coefficients can be evaluated in terms of factorials for integers or gamma functions in terms of real numbers

$$[-1]^j \binom{n}{j} = \binom{j-n-1}{j} = \frac{\Gamma(j-n)}{\Gamma(-n)\Gamma(j+1)}$$

Note that the binomial coefficients are now written in terms of gamma functions, therefore n can now be a real number. The n^{th} derivative is now written as

$$\frac{d^n f}{dx^n} \equiv \lim_{N \rightarrow \infty} \left\{ \left(\frac{x-a}{N} \right)^{-n} \sum_{j=0}^{N-1} \frac{\Gamma(j-n)}{\Gamma(-n)\Gamma(j+1)} f \left(x - j \left(\frac{x-a}{N} \right) \right) \right\} \quad (19)$$

2 1D Fractional Diffusion

2.1 A Numerical Approximation for the 1D Fractional Diffusion Equation

The following section is a description of a numerical scheme devised by Tadjeran [1] et al. It is a first order fractional scheme that aliases under the name of a second order scheme due to the implementation of Richardson extrapolation

The original code was written in FORTRAN, where the matrices and vectors start at position 1. The authors version was written in C++ where matrices and vectors start at position 0. Instead of shifting all indexes left in the algorithm, a decision was made to include the boundary conditions in the solution vector, hence the published indexes are left unchanged. The equation that is numerically approximated in ref[1] is the following;

$$\frac{\partial u(x,t)}{\partial t} = d(x) \frac{\partial^\alpha u}{\partial x^\alpha} + q(x,t) \quad (20)$$

$$\text{With } \begin{array}{ll} x_L < x < x_R & 1 < \alpha \leq 2, d(x) > 0 \\ u(x_L, t) = 0 & u(x_R, t) = b_R(t) \end{array} \quad u(x, t=0) = s(x)$$

The fractional operator used is the Right-shifted Grünwald formula and is used to estimate a spatial α -order fractional derivative[16]

$$\frac{\partial^\alpha u(x,t)}{\partial x^\alpha} = \frac{1}{\Gamma(-\alpha)} \lim_{N \rightarrow \infty} \frac{1}{h^\alpha} \sum_{k=0}^{k=N} \frac{\Gamma(k-\alpha)}{\Gamma(k+1)} u(x-h[k-1], t) \quad (21)$$

Or, in the same notation as equation 17, equation 19 becomes

$$\frac{\partial^\alpha u(x,t)}{\partial x^\alpha} = \lim_{N \rightarrow \infty} \frac{1}{h^\alpha} \sum_{k=0}^{k=N} \frac{\Gamma(k-\alpha)}{\Gamma(-\alpha)\Gamma(k+1)} u\left(x - \left[\frac{x-a}{N}\right][k-1], t\right)$$

Where N is a positive integer, $h = (x - x_L)/N$ and $\Gamma(*)$ is the gamma function.

The devised scheme applies the fractional derivative to the well known Crank-Nicholson scheme whereby the implicit and explicit schemes are averaged. Some definitions used here are $t_n = n\Delta t$ for $0 \leq t_n \leq T$, $\Delta x = h > 0$. $\Delta x = (x_R - x_L)/N_x$ with $x_i = x_L + i\Delta x$ for $i = 0$ to N_x , $d_i = d(x_i)$ and $q_i^{n+1/2} = q(x_i, t_{n+1/2})$.

The normalized Grünwald weights[12] are defined as

$$g_{\alpha,k} = \frac{\Gamma(k-\alpha)}{\Gamma(-\alpha)\Gamma(k+1)}$$

The first four terms in the sequence are given by

$$g_{\alpha,0} = 1, \quad g_{\alpha,1} = -\alpha, \quad g_{\alpha,2} = \frac{\alpha(\alpha-1)}{2!}, \quad g_{\alpha,3} = \frac{\alpha(\alpha-1)(\alpha-2)}{3!}.$$

When the approximate fractional derivative operator(21) is substituted into the Crank-Nicholson scheme the following is obtained.

$$\frac{U_i^{n+1} - U_i^n}{\Delta t} = \frac{d_i}{2} (\delta_{\alpha,x} U_i^{n+1} + \delta_{\alpha,x} U_i^n) + \frac{1}{2} (q_i^{n+1} + q_i^n) \quad (22)$$

Where the above fractional partial differential operator is defined as

$$\delta_{\alpha,x} U_i^n = \frac{1}{(\Delta x)^\alpha} \sum_{k=0}^N g_{\alpha,k} U_{i-k+1}$$

Equation (23) can be written in matrix form

$$\left(1 - \frac{d_i \Delta t}{2} \delta_{\alpha,x}\right) U_i^{n+1} = \left(1 + \frac{d_i \Delta t}{2} \delta_{\alpha,x}\right) U_i^n + \frac{1}{2} (q_i^{n+1} + q_i^n) \Delta t \quad (23)$$

$$\text{where } q_i^{n+1/2} \equiv \frac{1}{2} (q_i^{n+1} + q_i^n)$$

Equation (23) can be written in matrix form and solved in order to compute the vector U_i^{n+1} .

$$(I - A) \underline{U}^{n+1} = (I + A) \underline{U}^n + \underline{Q}^{n+1/2} \Delta t \quad (24)$$

where

$$\underline{U}^n = [U_0^n, U_1^n, \dots, U_{N-1}^n, U_N^n]^T$$

$$\underline{Q}^{n+1/2} = [q_0^{n+1/2}, q_1^{n+1/2}, \dots, q_{N-1}^{n+1/2}, q_N^{n+1/2}]^T$$

I is a $(N+1) \times (N+1)$ identity matrix

$$A_{i,j} = \begin{cases} \eta_i g_{i-j+1} & \text{for } j \leq i-1 \\ \eta_i g_1 & \text{for } j = i \\ \eta_i g_0 & \text{for } j = i+1 \\ 0 & \text{for } j > i+1 \end{cases}$$

$$\eta_i = \frac{d_i \Delta t}{2(\Delta x)^\alpha}$$

2.2 A 1D Numerical Example

The following problem is solved in Ref[1] and their results will be reproduced using the method described in Ref[1].

$$\frac{\partial u(x,t)}{\partial t} = d(x) \frac{\partial^{1.8} u}{\partial x^{1.8}} + q(x,t) \quad 0 \leq x \leq 1$$

$$d(x) = \Gamma(2.2)x^{2.8} / 6 = 0.183634x^{2.8} \quad \text{and} \quad q(x,t) = -(1+x)e^{-t}x^3$$

$$u(x,0) = x^3 \quad u(0,t) = 0 \quad u(1,t) = e^{-t}$$

The exact solution is $U(x,t) = e^{-t}x^3$ and can be verified by direct differentiation and substitution in the fractional diffusion equation using the formula

$$\frac{\partial^\alpha}{\partial x^\alpha} [x^p] = \frac{\Gamma(p+1)}{\Gamma(p+1-\alpha)} x^{p-\alpha}$$

Proof.

$$\frac{\partial u(x,t)}{\partial t} = d(x) \frac{\partial^{1.8} u}{\partial x^{1.8}} + q(x,t)$$

$$\therefore -e^{-t}x^3 = \frac{\Gamma(2.2)x^{2.8}}{6} e^{-t} \frac{\Gamma(3+1)}{\Gamma(3+1-1.8)} x^{1.2} - (1+x)e^{-t}x^3 \quad \{\Gamma(4) = 6\}$$

$$-e^{-t}x^3 = e^{-t}x^4 - (1+x)e^{-t}x^3$$

$$-e^{-t}x^3 = e^{-t}x^4 - e^{-t}x^3 - e^{-t}x^4$$

$$\therefore 0 = 0$$

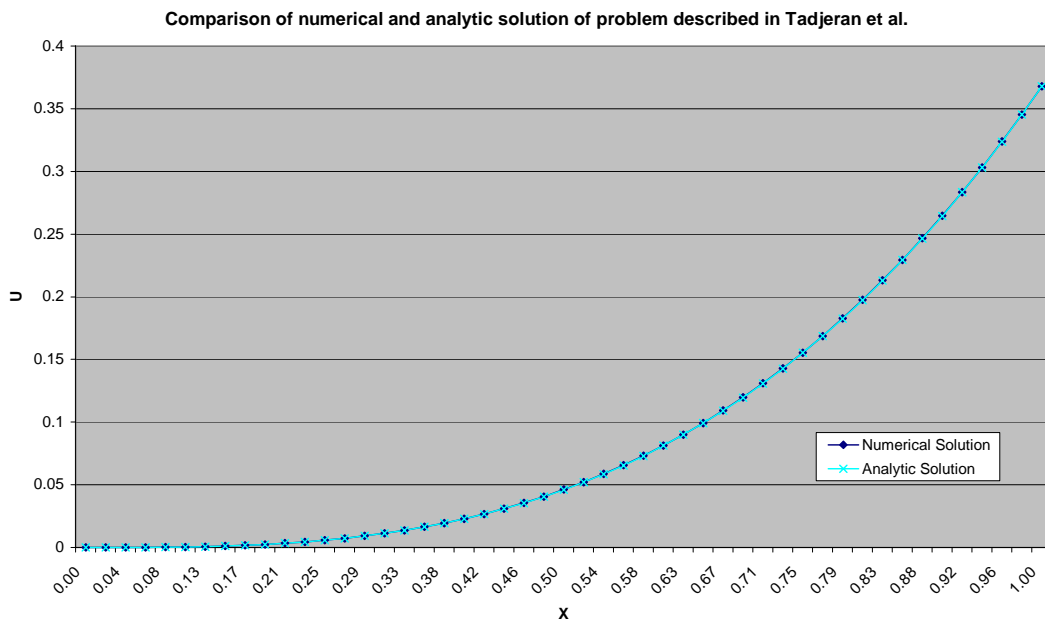


Fig 9 – Comparison of numerical and analytical solution. N=150, dt = 0.01.

dx	Max CN Error	Max Extrapolated Error
1/3	0.00545535	1.12E-05
1/6	0.00273296	2.82E-05
1/12	0.00136143	5.30E-06
1/24	0.00067994	1.72E-06
1/48	0.000340904	1.18E-06

Table 2 – Maximum Crank-Nicholson Error and Maximum Richardson Extrapolated Error

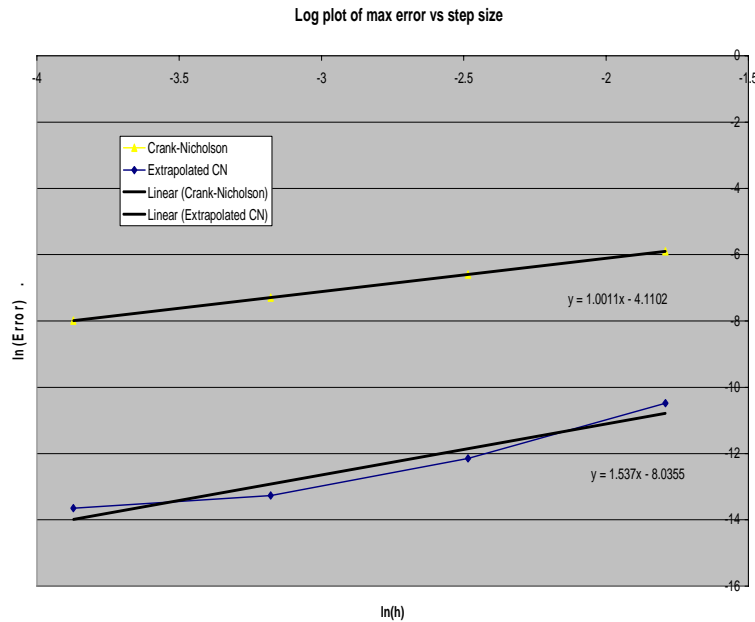


Fig 10 – log-log plot of maximum error of Crank-Nicholson and Extrapolated schemes vs step size. The gradient of the plots represents the order of accuracy of the scheme.

Tadgeran et al describe their scheme as first order in space for the Crank-Nicholson scheme and second order in space when the Richardson extrapolation is used. Figure 2 clearly shows that the order of accuracy for C-N is correct, however the statement that the extrapolated scheme is second order in space is not entirely correct as Tadgeran et al. base their error analysis on only four step sizes within the range $1/10 \leq h \leq 1/25$. The order of accuracy obtained with a step size with the range $1/3 \leq h \leq 1/50$ averages at about 1.5 and the order is clearly decreasing as the step size decreases. The order of accuracy is correct for the step sizes tested in Tadgeran et al, however, their analysis is flawed, as the Richardson extrapolation only works for relatively large step sizes.

2.3 Qualitative Behavior of Fractional Diffusive Systems

There are 3 basic definitions of fractional derivatives. The first two are left and right sided derivatives, which are based on the forward and backward Euler method respectively. The left and right sided definitions coincide with the standard integer derivatives. i.e. the method converges to the standard advection equation for $\alpha=1$ and the standard diffusion equation for $\alpha=2$. The symmetric definition is more artificial in a derivative sense as it does not coincide with the standard definition of a derivative and as its name suggests, the solution produced is symmetric and will not advect the solution for $\alpha < 2$.

$$\text{Symmetric} \quad \frac{d^\alpha f(x)}{d|x|^\alpha} = \begin{cases} -\frac{D_+^\alpha f(x) + D_-^\alpha f(x)}{2 \cos(\pi\alpha/2)}, & \alpha \neq 1 \\ -\frac{d}{dx} Hf(x), & \alpha = 1 \end{cases} \quad (25)$$

$$\text{Left} \quad D_+^\alpha f(x) = \frac{1}{\Gamma(2-\alpha)} \frac{d^2}{dx^2} \int_{-\infty}^x \frac{f(\xi, t) d\xi}{(x-\xi)^{\alpha-1}} \quad (26)$$

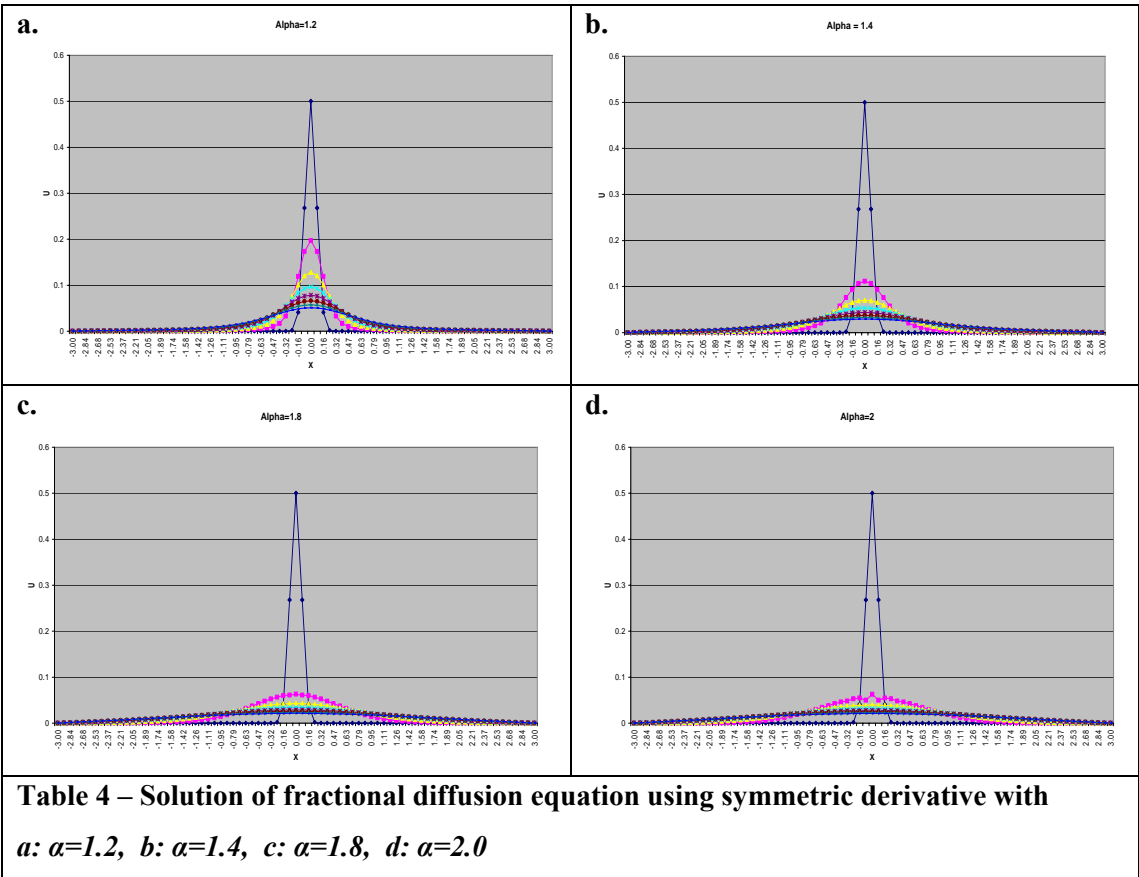
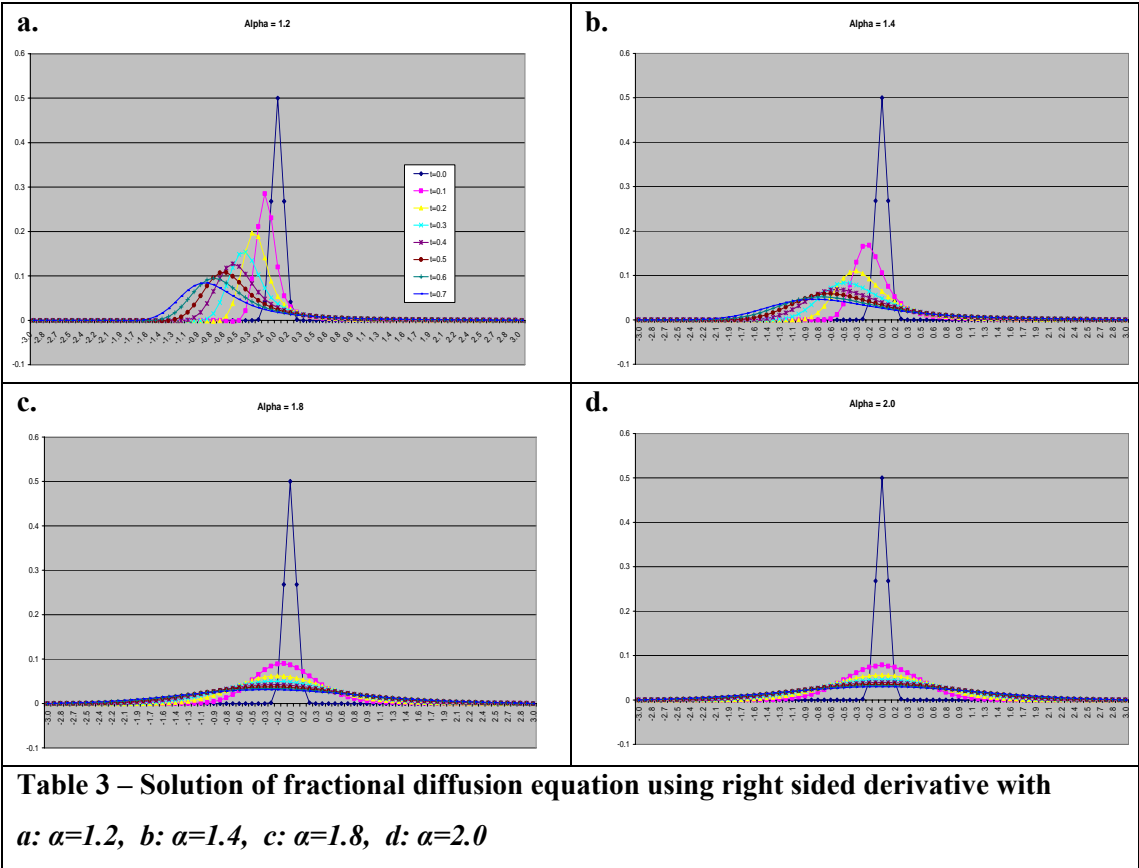
$$\text{Right} \quad D_-^\alpha f(x) = \frac{1}{\Gamma(2-\alpha)} \frac{d^2}{dx^2} \int_x^\infty \frac{f(\xi, t) d\xi}{(\xi-x)^{\alpha-1}} \quad (27)$$

Where H is defined as the Hilbert transform operator[27] and the left and right operators are the Riemann-Liouville derivatives.

$$Hf(x) = \frac{1}{\pi} \int_{-\infty}^{\infty} \frac{f(\xi) d\xi}{x-\xi} \quad (28)$$

It must be noted that the left and right derivative definitions (Eqn 26&27) when discretized, produce unstable methods for both implicit and explicit schemes [9]. It is for this reason that the right and left shifted Grünwald formulas are used to rectify this problem (c.f. Eqn 21).

The following few pages illustrate the differences in the solutions obtained from symmetric and non-symmetric derivatives. The iteration matrices(Matrix A in equation 24) are also shown.



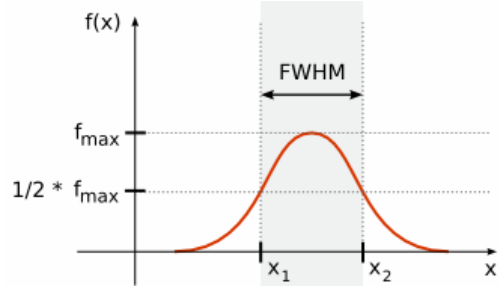
2.4 Full Width at Half Maximum

One method used to quantify the dispersive behavior of bell-like distributions is the Full Width at Half Maximum (FWHM).

This measurement can be used to quantify the speed of diffusion of the Gaussian wave with respect to different diffusive properties.

The following calculation predicts/verifies the evolution of the FWHM.

Starting with the fractional diffusion equation



$$\frac{\partial c(x,t)}{\partial t} = K \frac{\partial^\alpha c(x,t)}{\partial x^\alpha} \quad (29)$$

Take the Fourier transform to get

$$\frac{\partial \hat{c}(x,t)}{\partial t} = (ik)^\alpha K \hat{c}(k,t)$$

And solve to obtain

$$\hat{c}(k,t) = \exp^{Kt(ik)^\alpha}$$

Taking the inverse Fourier transform produces the spatial solution

$$c(x,t) = \frac{1}{\sqrt{4\pi Kt^\alpha}} \exp\left(\frac{-(x-x_o)^2}{4Kt^\alpha}\right)$$

This solution is a quasi-Gaussian and becomes a Gaussian when $\alpha=2$. To calculate the FWHM the maximum value must be found. This occurs when $\exp(*) = 1$.

$$\therefore c_{\max} = \frac{1}{\sqrt{4\pi Kt^\alpha}} \quad \text{and} \quad c_{\text{Half max}} = \frac{1}{2\sqrt{4\pi Kt^\alpha}} \quad (30)$$

Setting $x_o = 0$, FWHM is defined as the value of x where $c(x = FWHM, t) = c_{\text{Half max}}$.

$$\frac{1}{2\sqrt{4\pi Kt^\alpha}} = \frac{1}{\sqrt{4\pi Kt^\alpha}} \exp\left(\frac{-x^2}{4Kt^\alpha}\right)$$

$$\frac{1}{2} = \exp\left(\frac{-x^2}{4Kt^\alpha}\right)$$

$$x = FWHM = 2\sqrt{Kt^\alpha \ln(2)}$$

$$FWHM \propto t^{\alpha/2} \quad 1 < \alpha \leq 2$$

$\alpha=1$ is the advection equation which does not change the shape of the solution. Hence, for $\alpha=1$, $FWHM=0$.

The figure below proves the relation $FWHM \propto t^{\alpha/2}$ and $FWHM=0$ to be correct

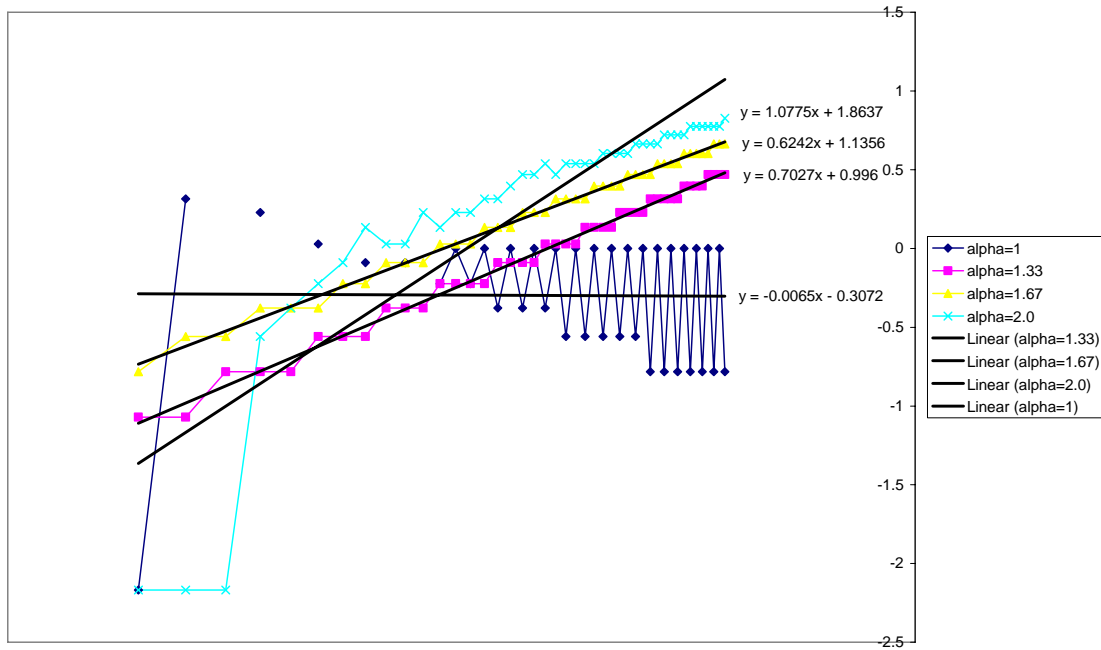


Fig 11 – A log-log plot of FWHM vs time. The gradient represents $\alpha/2$.
 $\alpha = 1$, gradient = **0.0065** $\alpha = 1.33$, gradient = **0.62**
 $\alpha = 1.67$, gradient = **1.67** $\alpha = 2.0$, gradient = **1.07**

2.5 Mean Square Deviation

Another method that can be used to quantify the rate of diffusion is the Mean Square Deviation(MSD). The following calculation derives equation (3) and its result can be used to predict/verify results.

The variance of $c(x,t)$ is readily obtained by applying the operator $\int_{-\infty}^{\infty} x^2 dx$ (the expectation value operator) to equation (29)

$$\frac{d}{dt} \langle x^2(t) \rangle = D \int_{-\infty}^{\infty} x^2 \frac{\partial^2 c(x,t)}{\partial x^2} dx$$

Integrating the RHS by parts twice and utilizing the normalization definition $\int_{-\infty}^{\infty} c(x,t)dx = 1$ gives the MSD relation for standard Brownian motion.

$$\langle x^2(t) \rangle = 2Dt \quad (31)$$

Note that for non-integer values of alpha the linear dependence of MSD on time is no longer holds. Proof:

$$\frac{\partial \langle c^2 \rangle}{\partial t} = K \frac{\partial^\alpha c}{\partial x^\alpha}$$

Applying the expectation value operator $\int_{-\infty}^{\infty} x^2 dx$ gives

$$\frac{\partial \langle c^2 \rangle}{\partial t} = K \int \frac{\partial^\alpha c}{\partial x^\alpha} x^2 dx$$

Integrating by parts twice gives

$$\frac{\partial \langle c^2 \rangle}{\partial t} = K \left[\frac{\partial^{\alpha-1} c}{\partial x^{\alpha-1}} x^2 \Big|_{-\infty}^{\infty} - 2x \frac{\partial^{\alpha-2} c}{\partial x^{\alpha-2}} \Big|_{-\infty}^{\infty} + 2 \frac{\partial^{\alpha-3} c}{\partial x^{\alpha-3}} \Big|_{-\infty}^{\infty} \right] \quad (32)$$

For alpha=2 the first two terms cancel. For alpha=1 there are three terms for which the first term is zero and the 2nd and 3rd cancel to give a MSD of zero. The last term for alpha=1 and alpha=2 is

$$2 \frac{\partial^{-1} c}{\partial x^{-1}} \Big|_{-\infty}^{\infty} = \int_{-\infty}^{\infty} c dx = 1 \quad (\text{Normalization condition})$$

Evaluating the integral then leaves equation 31.

For $1 < \alpha \leq 2$ the first terms do not cancel. To get the general idea of how the MSD will behave for $1 < \alpha < 2$ a particular solution of the diffusion equation is substituted into equation 32 and then integrating both sides w.r.t. time gives

$$c = \exp(-kt) \cdot \cos(\sqrt{kt})$$

$$\langle c^2 \rangle = \int_0^T K \left[\frac{\partial^{\alpha-1} \exp(-kt) \cdot \cos(\sqrt{kt})}{\partial x^{\alpha-1}} \Big|_{-\infty}^{\infty} x^2 - \frac{\partial^{\alpha-2} \exp(-kt) \cdot \cos(\sqrt{kt})}{\partial x^{\alpha-2}} \Big|_{-\infty}^{\infty} 2x + 2 \frac{\partial^{\alpha-3} \exp(-kt) \cdot \cos(\sqrt{kt})}{\partial x^{\alpha-3}} \Big|_{-\infty}^{\infty} \right] dt$$

For alpha=1.5, the MSD becomes

$$\langle c^2 \rangle = \int_0^T K \left[\frac{\partial^{1/2} \exp(-kt) \cdot \cos(\sqrt{kt})}{\partial x^{1/2}} \Big|_{-\infty}^{\infty} x^2 - \frac{\partial^{-1/2} \exp(-kt) \cdot \cos(\sqrt{kt})}{\partial x^{-1/2}} \Big|_{-\infty}^{\infty} 2x + 2 \frac{\partial^{-3/2} \exp(-kt) \cdot \cos(\sqrt{kt})}{\partial x^{-3/2}} \Big|_{-\infty}^{\infty} \right] dt$$

Hence the MSD is now a combination of semi-derivatives, semi-integrals and a 3/2 ordered integral. Producing an analytic solution of this equation a fairly tricky, but intuition tells me that the solution to this equation will reduce to a fairly simple equation

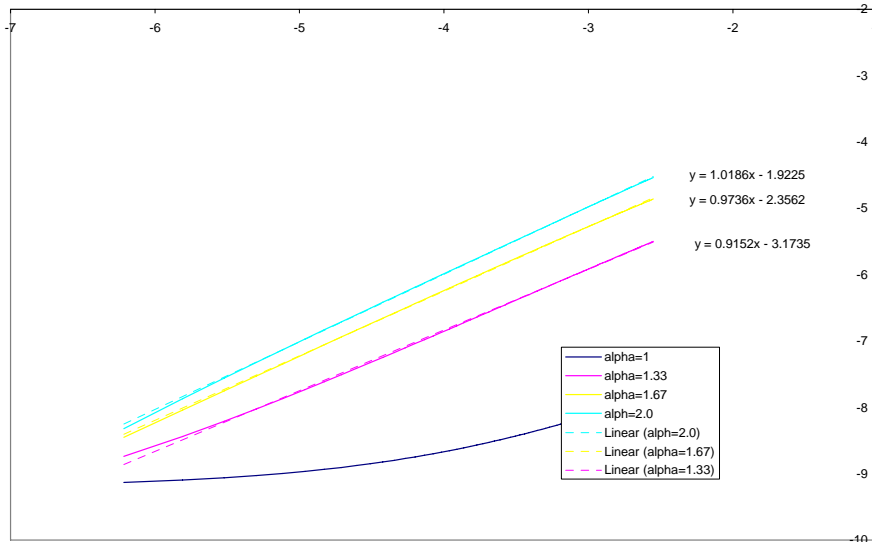


Fig 12 – The MSD symmetric fractional diffusion for $\alpha = 1, 1.33, 1.67$ and 2.0 . The blue line ($\alpha = 2$) shows linear dependence on time. The yellow line ($\alpha = 1.67$) shows a gradient of 0.97 (slightly sub diffusive). The pink line ($\alpha = 1.33$) shows a gradient of 0.91 (still only slight subdiffusion) while the dark blue line ($\alpha = 1$) shows non linear behaviour.

2.6 Iteration Matrices

The iteration matrix, A, in equation 24 is based on the right sided fractional derivative and is defined as

$$A_{i,j} = \begin{cases} \eta_i g_{i-j+1} & \text{for } j \leq i-1 \\ \eta_i g_1 & \text{for } j = i \\ \eta_i g_0 & \text{for } j = i+1 \\ 0 & \text{for } j > i+1 \end{cases}$$

$$\eta_i = \frac{d_i \Delta t}{2(\Delta x)^\alpha}$$

The link between super diffusion and fractional derivatives is the wide stencil of the fractional scheme that allows enhanced mixing. The standard diffusion stencil takes into account only three points, whereas the right sided stencil can be composed of upto $N/2+1$ points (N is total number of points) .

The iteration matrix needed to describe the symmetric derivative as described in equation 26 is defined as

$$A_{i,j} = \begin{cases} \eta_i g_{i-j+1} & \text{for } j < i-1 \\ 2\eta_i g_1 & \text{for } j = i \\ \eta_i (g_0 + g_2) & \text{for } j = i+1 \\ \eta_i g_{i+j-1} & \text{for } j > i+1 \\ \eta_i (g_0 + g_2) & \text{for } j = i-1 \end{cases}$$

The symmetric stencil is as large as a stencil can be, as its width is the size of the domain. The right-sided derivative operator only diffused to the left. Whereas the symmetric operator diffuses equally in both directions. The width of the stencil determines the speed at which the initial conditions will diffuse/mix. A large stencil will allow a large peak to interact with a negligible value that is far away from the peak and the opposite also occurs whereby a negligible value will mix with a high peak which would not occur in the standard stencil.

When the derivative order is an integer value the stencil reduces to 3 points, hence the diffusion for integer alpha is standard diffusion. As the value of alpha moves away from an integer value the stencil increases and the diffusion becomes more/less diffusive. Table 4 proves non-integer α to be less diffusive.

The following pages show the iteration matrices for alpha= 1, 1.5 and 2 for both right sided and symmetric cases.

$$\alpha = 1$$

A2Right Grunwald Weights

0	0	0	0	0	0	0	0	0
0	-1	1	0	0	0	0	0	0
0	0	-1	1	0	0	0	0	0
0	0	0	-1	1	0	0	0	0
0	0	0	0	-1	1	0	0	0
0	0	0	0	0	-1	1	0	0
0	0	0	0	0	0	-1	1	0
0	0	0	0	0	0	0	-1	1
0	0	0	0	0	0	0	0	0

A2symmetric Grunwald Weights

0	0	0	0	0	0	0	0	0
0	-1	2	-1	0	0	0	0	0
0	0	-1	2	-1	0	0	0	0
0	0	0	-1	2	-1	0	0	0
0	0	0	0	-1	2	-1	0	0
0	0	0	0	0	-1	2	-1	0
0	0	0	0	0	0	-1	2	-1
0	0	0	0	0	0	0	-1	2
0	0	0	0	0	0	0	0	0

$$\alpha = 1.5$$

A2Right Grunwald Weights

0	0	0	0	0	0	0	0	0
0.375	-1.5	1	0	0	0	0	0	0
0.0625	0.375	-1.5	1	0	0	0	0	0
0.023438	0.0625	0.375	-1.5	1	0	0	0	0
0.011719	0.023438	0.0625	0.375	-1.5	1	0	0	0
0.006836	0.011719	0.023438	0.0625	0.375	-1.5	1	0	0
0.004395	0.006836	0.011719	0.023438	0.0625	0.375	-1.5	1	0
0.003021	0.004395	0.006836	0.011719	0.023438	0.0625	0.375	-1.5	1
0	0	0	0	0	0	0	0	0

A2symmetric Grunwald Weights

0	0	0	0	0	0	0	0	0
0.972272	-2.12132	0.972272	0.044194	0.016573	0.008286	0.004834	0.003107	0.002136
0.044194	0.972272	-2.12132	0.972272	0.044194	0.016573	0.008286	0.004834	0.003107
0.016573	0.044194	0.972272	-2.12132	0.972272	0.044194	0.016573	0.008286	0.004834
0.008286	0.016573	0.044194	0.972272	-2.12132	0.972272	0.044194	0.016573	0.008286
0.004834	0.008286	0.016573	0.044194	0.972272	-2.12132	0.972272	0.044194	0.016573
0.003107	0.004834	0.008286	0.016573	0.044194	0.972272	-2.12132	0.972272	0.044194
0.002136	0.003107	0.004834	0.008286	0.016573	0.044194	0.972272	-2.12132	0.972272
0	0	0	0	0	0	0	0	0

$$\underline{\alpha = 2}$$

A2Right Grunwald Weights

0	0	0	0	0	0	0	0	0
1	-2	1	0	0	0	0	0	0
0	1	-2	1	0	0	0	0	0
0	0	1	-2	1	0	0	0	0
0	0	0	1	-2	1	0	0	0
0	0	0	0	1	-2	1	0	0
0	0	0	0	0	1	-2	1	0
0	0	0	0	0	0	1	-2	1
0	0	0	0	0	0	0	0	0

A2symmetric Grunwald Weights

0	0	0	0	0	0	0	0	0
1	-2	1	0	0	0	0	0	0
0	1	-2	1	0	0	0	0	0
0	0	1	-2	1	0	0	0	0
0	0	0	1	-2	1	0	0	0
0	0	0	0	1	-2	1	0	0
0	0	0	0	0	1	-2	1	0
0	0	0	0	0	0	1	-2	1
0	0	0	0	0	0	0	0	0

2.7 Fractional Fokker-Planck Equation

The standard Fokker-Planck {named after Adriaan Fokker and Max Planck[13]} equation(33) is a dynamic equation that describes the evolution of a probability density distribution, $P(x,t)$, of a continuous time random walk(Brownian) in the presence of an external force field.

$$\frac{\partial}{\partial t} P(x,t) = \left(-\frac{\partial}{\partial x} \frac{F(x)}{m\eta} + K \frac{\partial^2}{\partial x^2} \right) P(x,t) \quad (33)$$

Where $F=-dV/dx$, m is the mass of the diffusing material and η is viscosity/friction coefficient.

The fractional Fokker-Planck equation(34)[12] is a variation of the standard equation whereby the order of the derivative associated with diffusion in the standard equation can now take a non-integer value. The fFPE describes the behavior of Levy flights in potentials.

$$\frac{\partial}{\partial t} P(x,t) = \left(-\frac{\partial}{\partial x} \frac{F(x)}{m\eta} + K^{(\alpha)} \frac{\partial^\alpha}{\partial |x|^\alpha} \right) P(x,t) \quad (34)$$

Note that the symmetric derivative operator is now employed in the diffusive term to ensure that $1 \leq \alpha < 2$ contributes only to diffusive behavior, whereas a right or left sided derivate for this range of α would cause a combination of advection and diffusion.

The exact solution solution of (asd) with no forcing term can be solved easily in Fourier space as the Levy stable density $P(k,t) = \exp(-K^{(\alpha)} |k|^\alpha t)$. However, when this solution is transformed back into position space the solution is given in terms of Fox H functions[12].

$$P(x,t) = \frac{1}{\alpha |x|} H_{2,2}^{1,1} \left[\frac{|x|}{(K^{(\alpha)} t)^{1/\alpha}} \middle| \begin{matrix} (1,1/\alpha), (1,1/2) \\ (1,1), (1,1/2) \end{matrix} \right]$$

The notation of (34) is somewhat misleading, as one would assume that the differential operator would act upon the $F(x)$ term and the $P(x)$ and would result in chain rule differentiation. However, the results shown in references 10 and 12 prove otherwise, as their results are symmetric. If the differential operator was to act on $P(x,t)$ as well as $F(x)$, the solution would advect and the line of symmetry associated with the force field will no longer coincide with that of the solution, resulting in the solution becoming non-symmetric.

2.5.1 Presence of Quartic Potential

The quartic potential(37) is a high order harmonic potential, which in this case is used to investigate the behavior of levy flights in the presence of steep potentials[10,12].

$$V(x) = \frac{a}{2}x^2 + \frac{b}{4}x^4 \quad (35)$$

Figures 13 & 14 below compare the authors result with the result from Metzler et al where the problem was initially discussed.

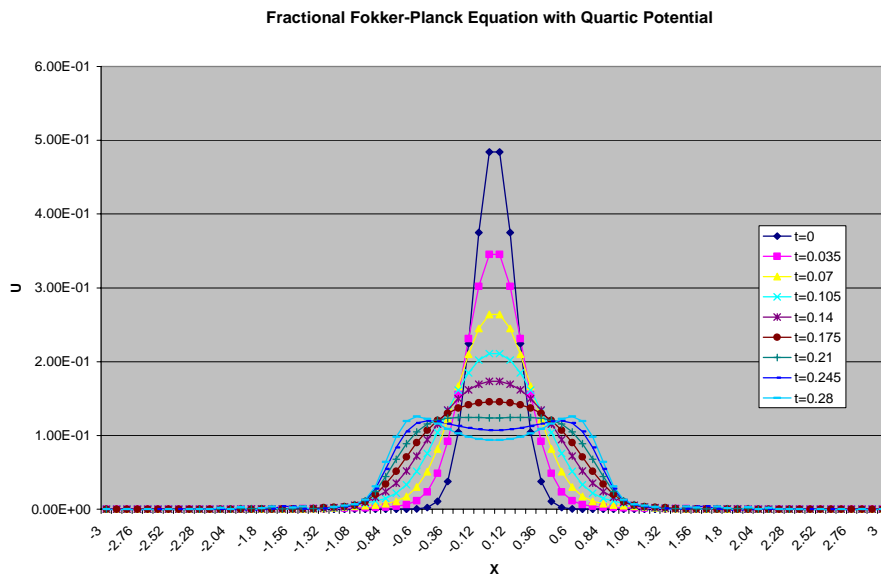


Fig 13 – Solution of eqn 35 with quartic potential(37).

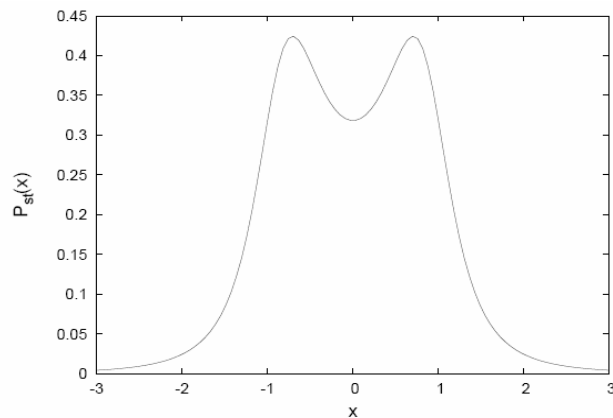


Fig 14 [12]- Stationary solution of equation 35 in Tadjeran et al.

2.5.2 Fractional Fokker-Planck with Superharmonic potential

The superharmonic potential is defined as[10,12]

$$V(x) = \frac{a}{c} |x|^c \quad (36)$$

Figures 10 & 11 below show the comparison of the authors solution with that of Metzler et al.

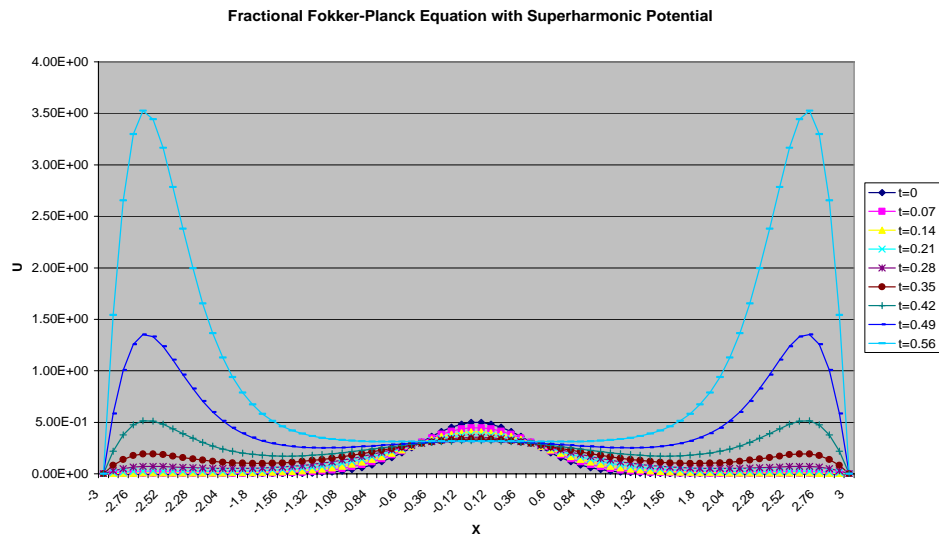


Fig 15 – Solution of the eqn 35 with superharmonic potential(eq. 36).

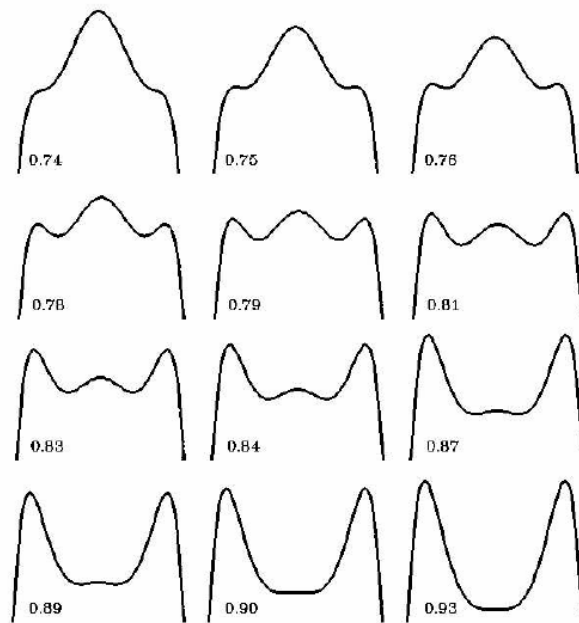


Fig 16 [10] – The solution of the Fractional Fokker-Planck equation with superharmonic potential presented in Metzler et al.

3 2D Fractional Diffusion

3.1 A Numerical Approximation for the 2D Fractional Diffusion Equation

This next section is a succinct version of ref[11] that will describe an algorithm for solving the 2D fractional diffusion equation.

$$\frac{\partial u(x, y, t)}{\partial t} = d(x, y) \frac{\partial^\alpha u(x, y, t)}{\partial x^\alpha} + e(x, y) \frac{\partial^\alpha u(x, y, t)}{\partial x^\alpha} + q(x, y, t) \quad (37)$$

As with the 1D example, the 2D case is based on a paper by Tadjeran and Meerschart[11] which uses a Crank-Nicholson theory applied to the right shifted Grunwald formula(eqn 21). The use of Richardson extrapolation is also used to enable the primarily first order accurate scheme to become second order accurate in time and space. Equation 14 in the 1D example when extended to 2D becomes

$$\frac{U_i^{n+1} - U_i^n}{\Delta t} = \frac{1}{2} (\delta_{\alpha,x} U_{i,j}^{n+1} + \delta_{\alpha,x} U_{i,j}^n + \delta_{\beta,y} U_{i,j}^{n+1} + \delta_{\beta,y} U_{i,j}^n) + \frac{1}{2} (q_{i,j}^{n+1} + q_{i,j}^n) \quad (38)$$

The above fractional partial differential operators are slightly different in 2D and are defined as

$$\delta_{\alpha,x} U_{i,j}^n = \frac{d_{i,j}}{(\Delta x)^\alpha} \sum_{k=0}^{i+1} g_{\alpha,k} U_{i-k+1,j}$$

$$\delta_{\beta,y} U_{i,j}^n = \frac{e_{i,j}}{(\Delta x)^\alpha} \sum_{k=0}^{j+1} g_{\alpha,k} U_{i,j-k+1}$$

Equation (38) can be written in matrix form

$$\left(1 - \frac{\Delta t}{2} \delta_{\alpha,x} - \frac{\Delta t}{2} \delta_{\beta,y} \right) U_i^{n+1} = \left(1 + \frac{\Delta t}{2} \delta_{\alpha,x} + \frac{\Delta t}{2} \delta_{\beta,y} \right) U_i^n + \frac{1}{2} (q_i^{n+1} + q_i^n) \Delta t \quad (39)$$

Or in matrix form,

$$(I - A - B)U^{n+1} = (I + A + B)U^n + Q^{n+1/2} \Delta t \quad (40)$$

Equation (40) can be solved in the same way as 1D case by multiplying both sides by $(I - A - B)^{-1}$, although this method is very computationally expensive and inefficient due to the sparse nature of the matrix to be inverted. One way around this is to use the alternating directions implicit (ADI) method to reduce the computational work. This method works by introducing a perturbation of Eqn (40) and solving the equation explicitly in one direction and implicitly in the other. This method creates a system of matrix equations whereby an

intermediate solution is defined and is to be solved and then substituted into the second equation to define the final solution.

$$(I - A)\underline{U}_{i,j}^* = (I + B)\underline{U}_{i,j}^n + \frac{\Delta t}{2}\underline{Q}^{n+1/2} \quad (41)$$

$$(I - B)\underline{U}_{i,j}^{n+1} = (I + A)\underline{U}_{i,j}^* + \frac{\Delta t}{2}\underline{Q}^{n+1/2} \quad (42)$$

Where

$$\underline{U}^n = [U_0^n, U_1^n, \dots, U_{N-1}^n, U_N^n]^T$$

$$\underline{Q}^{n+1/2} = [q_0^{n+1/2}, q_1^{n+1/2}, \dots, q_{N-1}^{n+1/2}, q_N^{n+1/2}]^T$$

I is a $(N + 1) \times (N + 1)$ identity matrix

$$A_{i,j} = \begin{cases} D_{i,k} g_{\alpha, i-j+1} & \text{for } j \leq i-1 \\ D_{i,k} g_{\alpha, 1} & \text{for } j = i \\ D_{i,k} g_{\alpha, 0} & \text{for } j = i+1 \\ 0 & \text{for } j > i+1 \end{cases}$$

$$B_{i,j} = \begin{cases} E_{i,k} g_{\beta, i-j+1} & \text{for } j \leq i-1 \\ E_{i,k} g_{\beta, 1} & \text{for } j = i \\ E_{i,k} g_{\beta, 0} & \text{for } j = i+1 \\ 0 & \text{for } j > i+1 \end{cases}$$

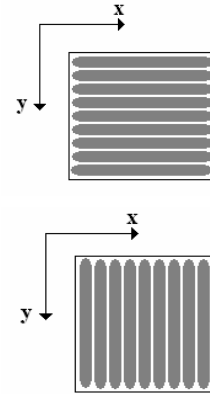
$$A_{0,0} = B_{0,0} = A_{N,N} = B_{N,N} = 1$$

$$E_{i,k} = \frac{e_i \Delta t}{2(\Delta y)^\beta}$$

$$D_{i,k} = \frac{d_i \Delta t}{2(\Delta x)^\alpha}$$

The algorithm for implemented in the following way:

1. Solve on each horizontal slice $y=y_k$ ($k=1..N_y-1$), a set of N_x-1 equations defined by (22) to obtain the intermediate solution U^* .
2. Next, solve on each vertical slice $x=x_k$ ($k=1..N_y-1$), a set of N_y-1 equations defined by (23) to obtain the solution slice U^{n+1}



The boundary conditions needed to maintain consistency of equation

(40) are

$$2U_{i,j}^* = \left(1 - \frac{\Delta t}{2} \delta_{\beta,y}\right) U_{i,j}^{n+1} + \left(1 + \frac{\Delta t}{2} \delta_{\beta,y}\right) U_{i,j}^n \quad (43)$$

This (24) can be derived by subtracting eqn (42) from equation (41)

$$U_{0,j}^* = \frac{1}{2} \left[\left(1 - \frac{\Delta t}{2} \delta_{\beta,y}\right) U_{0,j}^{n+1} + \left(1 + \frac{\Delta t}{2} \delta_{\beta,y}\right) U_{0,j}^n \right]$$

$$U_{N,j}^* = \frac{1}{2} \left[\left(1 - \frac{\Delta t}{2} \delta_{\beta,y}\right) U_{N,j}^{n+1} + \left(1 + \frac{\Delta t}{2} \delta_{\beta,y}\right) U_{N,j}^n \right]$$

3.2 A 2D Numerical Example

The following problem is solved in [11] and their results are reproduced here.

$$\frac{\partial u(x, y, t)}{\partial t} = d(x, y) \frac{\partial^\alpha u(x, y, t)}{\partial x^\alpha} + e(x, y) \frac{\partial^\alpha u(x, y, t)}{\partial x^\alpha} + q(x, y, t) \quad 0 \leq x, y \leq 1 \quad (44)$$

$$d(x) = \Gamma(2.2)x^{2.8}y/6 \quad e(x) = 2x y^{2.6} / \Gamma(4.6)$$

$$u(0, y, t) = 0 \quad u(x, 0, t) = 0$$

$$u(x, 1, t) = e^{-t}x^3 \quad u(1, y, t) = e^{-t}y^{3.6}$$

$$q(x, t) = -(1 + 2xy)e^{-t}x^3y^{3.6} \quad \alpha=1.8, \beta=1.6$$

The exact solution is $u(x, y, t) = e^{-t}x^3y^{3.6}$ and can be verified by direct differentiation and substitution in the fractional diffusion equation using the formula

$$\frac{\partial^\alpha}{\partial x^\alpha} [x^p] = \frac{\Gamma(p+1)}{\Gamma(p+1-\alpha)} x^{p-\alpha}$$

Proof.

$$\frac{\partial}{\partial t} [e^{-t}x^3y^{3.6}] = \frac{\Gamma(2.2)x^{2.8}y}{6} \frac{\partial^{1.8}}{\partial x^{1.8}} [e^{-t}x^3y^{3.6}] + \frac{2xy^{2.6}}{\Gamma(4.6)} \frac{\partial^{1.6}}{\partial y^{1.6}} [e^{-t}x^3y^{3.6}] - (1 + 2xy)e^{-t}x^3y^{3.6}$$

$$\therefore -e^{-t}x^3y^{3.6} = \frac{\Gamma(2.2)x^{2.8}y}{6} \frac{\Gamma(3+1)}{\Gamma(3+1-1.8)} e^{-t}x^{1.2}y^{3.6} + \frac{2xy^{2.6}}{\Gamma(4.6)} \frac{\Gamma(4.6)}{\Gamma(4.6-1.6)} e^{-t}x^3y^{3.6} - (1 + 2xy)e^{-t}x^3y^{3.6}$$

$$-x^3 = yx^4 + \frac{2x^4y}{\Gamma(3)} - (1 + 2xy)x^3 \quad \{\Gamma(4) = 6\} \quad \{\Gamma(3) = 2\}$$

$$-1 = xy + xy - 1 - 2xy$$

$$\therefore 0 = 0$$

dt	dx	Max CN Error
1/100	1/5	3.21E-03
1/100	1/10	1.67E-03
1/100	1/20	8.03E-04
1/100	1/40	4.01E-04

Table 2 – Maximum Crank-Nicholson Error and Maximum Richardson Extrapolated Error.

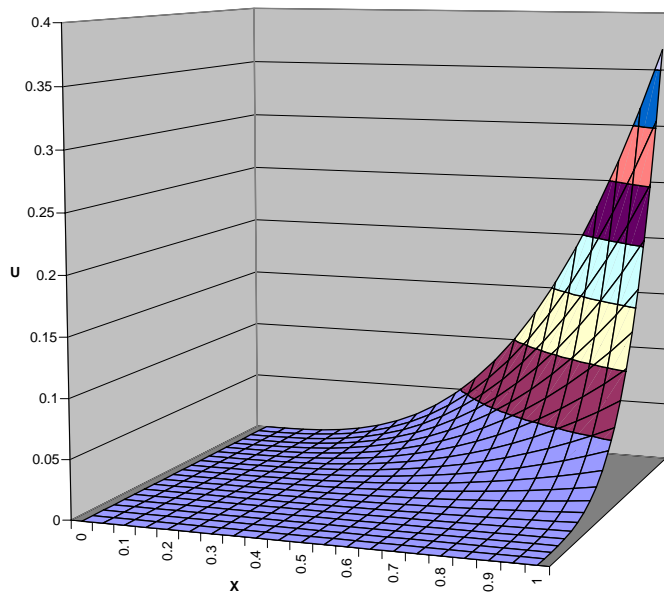


Fig 17 – The computed solution to eqn 44 using the first order accurate method described above.

Table 2 clearly shows linear error convergence, as the halving a step size halves the maximum absolute error.

3.3 2D Diffusion

The fractional diffusion equation in the previous example is based on the right sided derivative which is derived from the same theory as the backwards Euler method. The problem with this derivative, when applied to diffusion, is that it only diffuses in one direction for $1 \leq \alpha < 2$, or to be more pedantic it advects to the left and diffuses at the same time. This is not realistic as standard diffusion causes the prognostic variable to spread equally in all directions. As a result the standard method to simulate diffusion makes use of the symmetric derivative (eqn asdfgh). The fractional diffusion equation in 2D is defined as

$$\frac{\partial U}{\partial t} = \frac{\partial^\alpha U}{\partial |x|^\alpha} + \frac{\partial^\beta U}{\partial |y|^\beta} + S(x, y)$$

The following pages show the behaviour of a 2D Gaussian function undergoing symmetric fractional diffusion on a domain $x, y \in [-1, 1]$ in the interval $t \in [0, 1]$. The simulation is based on initial conditions of

$$U(x, y, t = 0) = 0.5 \exp\left(-\frac{x^2 + y^2}{0.1}\right)$$

with $dx=dy = 1/60$ and $dt=0.01$.

and boundary conditions of

$$U(-1, y, t) = U(x, -1, t) = 0$$

$$U(1, y, t) = U(x, 1, t) = 0$$

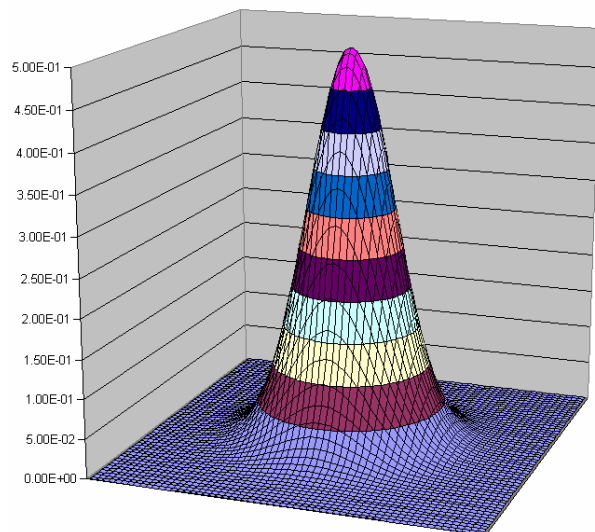


Fig 18 – Initial condition for 2D symmetric diffusion.

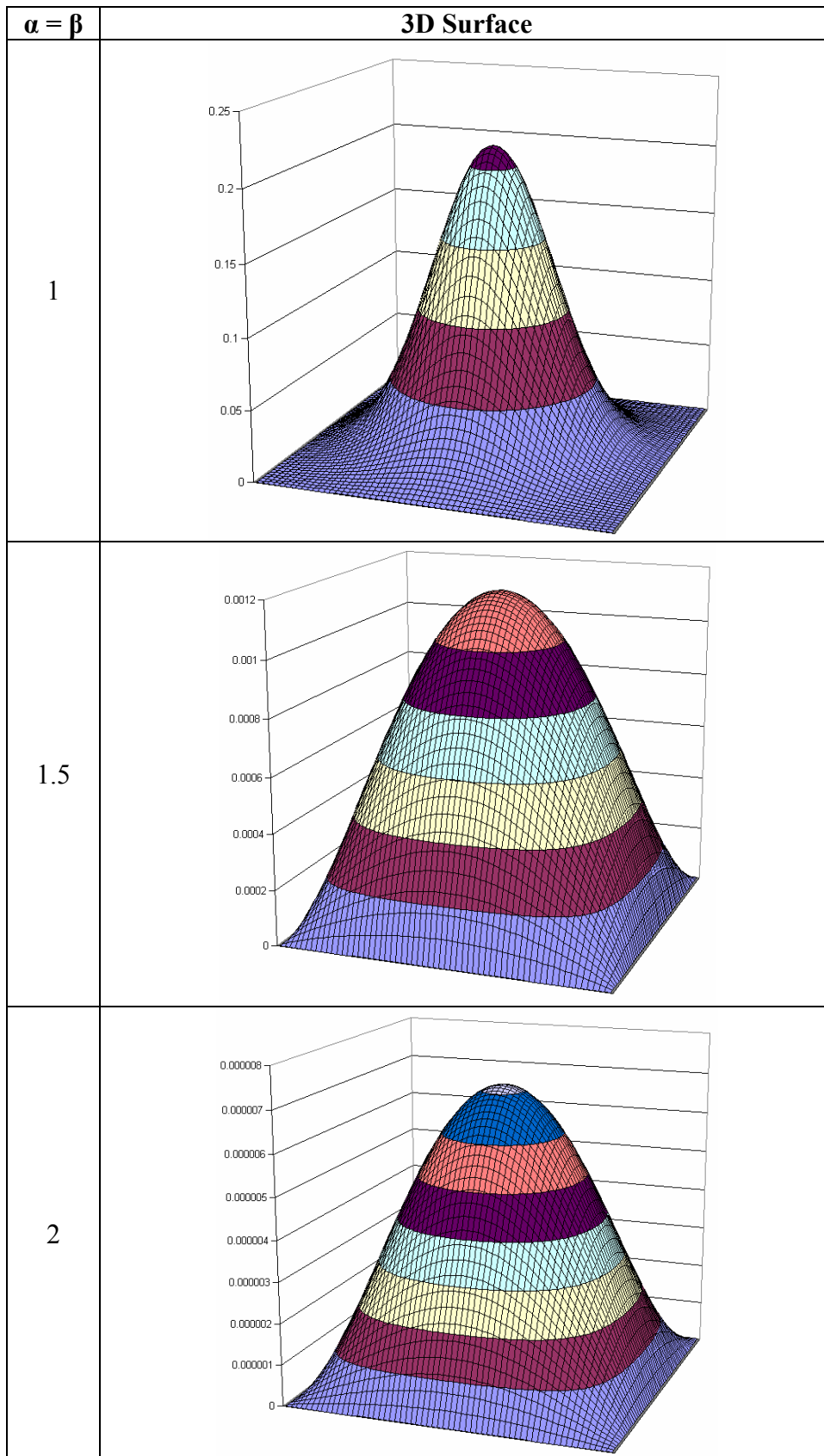
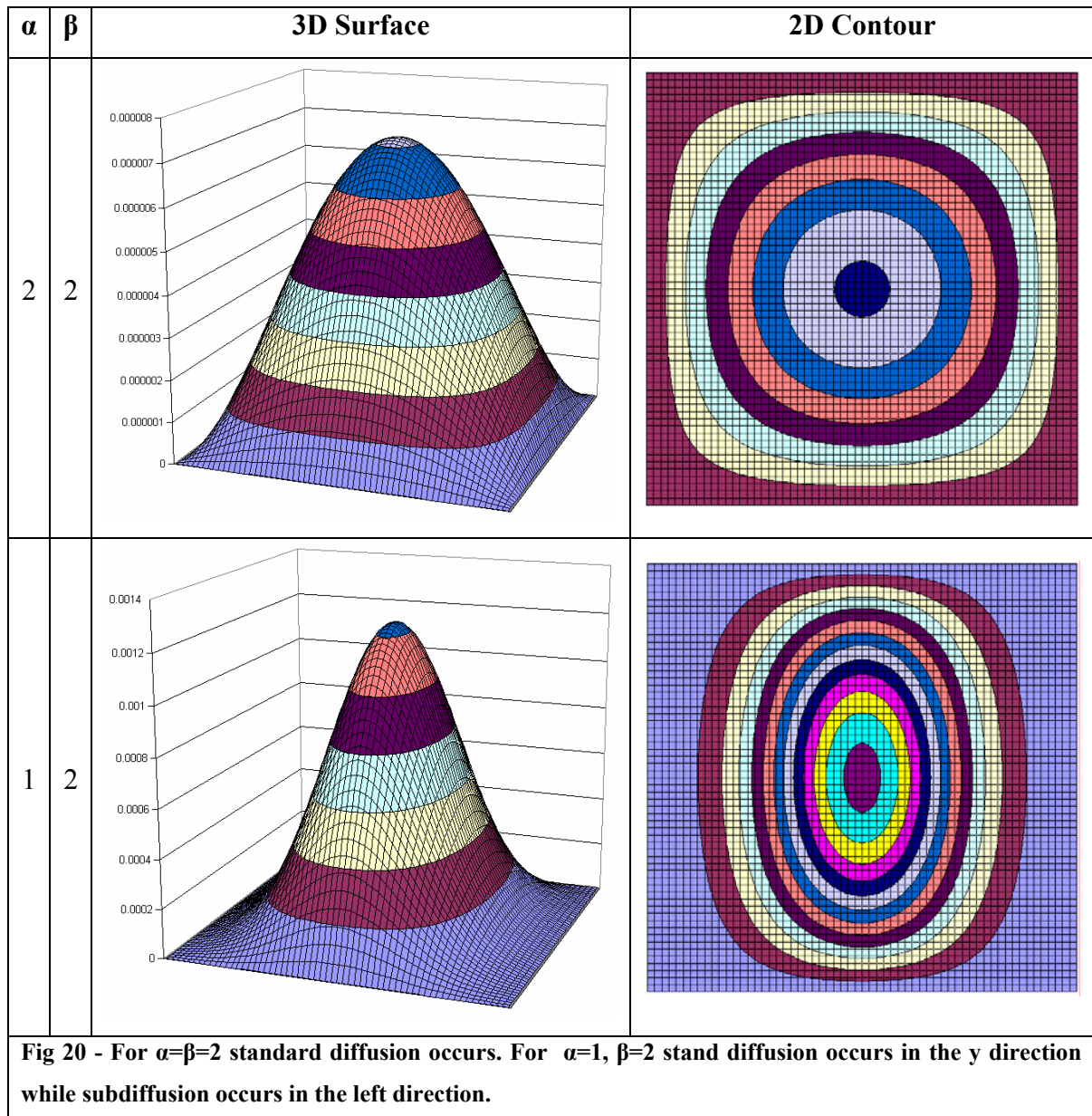


Fig 19 – The 3D Gaussian profiles after undergoing fractional diffusion for 1 second. Pay attention to the scales on the graphs as there is a significant difference between $\alpha=1$ and $\alpha=2$. Also note the shape of the Gaussian shape is slightly different (steeper at edges) for each of them due to the Gaussian wanting to spread but not being able to due to the Dirichlet b.c.'s.

3.4 Skewed Diffusion

Skewed diffusion occurs when diffusion is more prominent on one direction. One real life example of this is the percolation of water in the water table where the rocks are formed in layers and the diffusion is more prevalent in the direction that is parallel to these layers. The simulations below compare skewed and non-skewed diffusion.



4 2D Plume Diffusion

Anomalous diffusion of tracers(contaminants) has been observed whereby turbulence causes the tracers to diffuse with non-Gaussian behaviour. The aim of this section is to reproduce the empirical phenomena using 2D fractional diffusion.

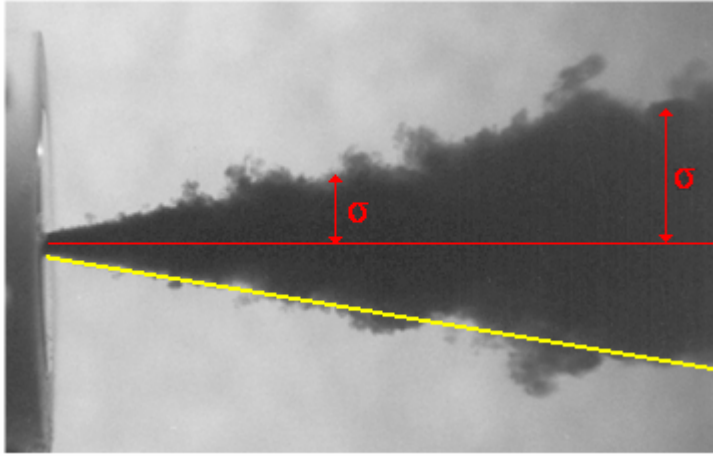


Fig 17 – The plume diffusion shows a nonlinear spread that is characteristic of super diffusion. The variance of the plume has a linear relation with time for standard diffusion.

The model needed to reproduce the anomalous plume diffusion is the fractional advection diffusion equation.

$$\frac{\partial U}{\partial t} + v \frac{\partial U}{\partial x} = K_{\beta}^y \frac{\partial^{\beta} U}{\partial y^{\beta}} \quad (45)$$

Where U is the density of the tracer, v is its velocity in the x direction and K_{β}^y is the diffusivity in the y direction.

Results

The following contour plots illustrate the effect that differential exponent has on the dispersion of a tracer. A Gaussian shaped tracer is introduced to the domain on the left hand side. The tracer is then advected in the x direction while being fractionally diffused in the y direction. The aim of this simulation is to produce contour plots that resemble the plume diffusion shown above.

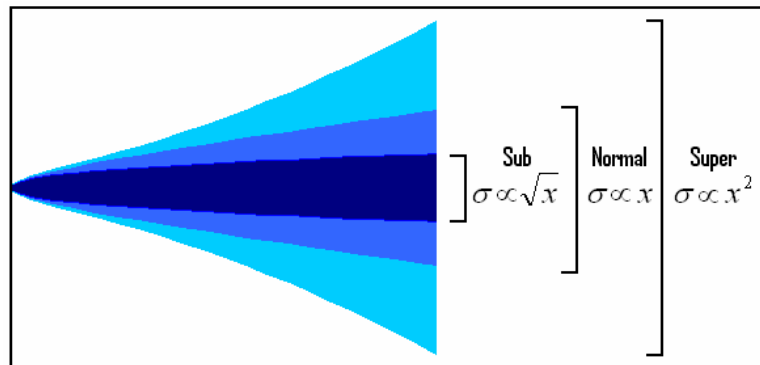


Fig 18 – Idealised tracer dispersion in the case of sub, normal and super diffusion.

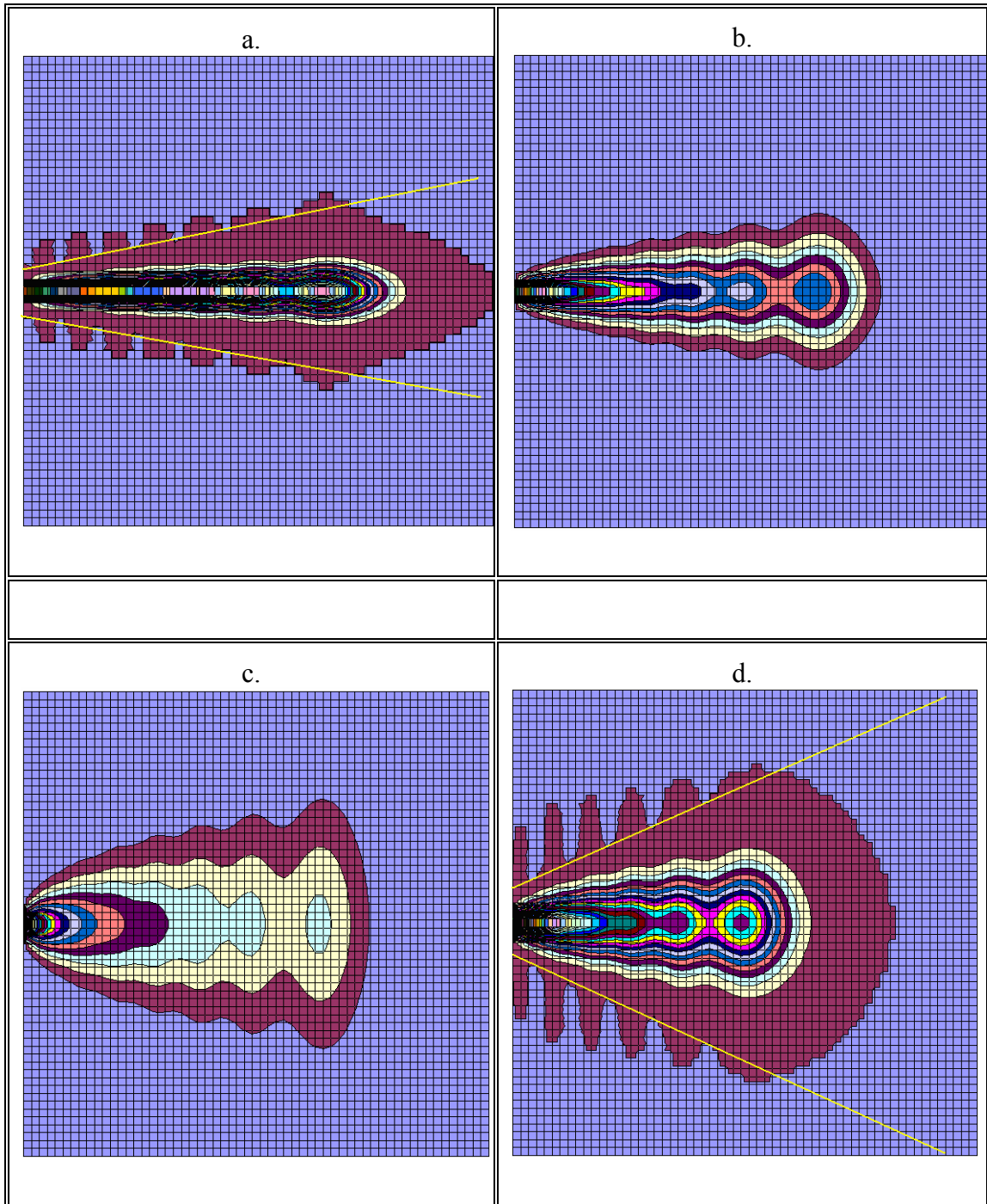


Fig 19 – Figur showing the the spread of as tracer which is under the influence of advection and fractional diffusion. a: $\alpha=1$, b: $\alpha=1.33$, c: $\alpha=1.67$, d: $\alpha=2.0$. a & d show a linear spread which characterises normal diffuson. b & c show non linear(similar to square root) behaviour that is of a sub diffusive nature.

5 Functional Order Derivatives

5.1 An Extension of Fractional Derivatives

The concept of functional derivatives is well known [33,34,35] and forms a branch of variational calculus. The functional derivative differs from a standard derivative as it does not differentiate w.r.t a variable as in the standard case, instead it differentiates w.r.t. a function. In physics the function with which the subject function is differentiated with respect to is often a vector. The definition is [36]

$$\frac{\partial F[f(x)]}{\partial f(y)} = \lim_{\varepsilon \rightarrow 0} \frac{F[f(x) + \varepsilon \delta(x-y)] - F[f(x)]}{\varepsilon}$$

One variation of a functional derivative which has not yet been explored is the concept of *functional order derivatives* (FOD). Descriptively, this is the differentiation of order $f(x)$ of a function $F(x)$. Using the (left) Riemann definition of a fractional derivative, the functional order derivative is defined as

$$\frac{d^{g(f,x,t)} f}{dx^{g(f,x,t)}} \equiv \lim_{\Delta x \rightarrow 0} \left\{ [\Delta x]^{-g(f,x,t)} \sum_{j=0}^{N-1} [-1]^j \binom{g(f,x,t)}{j} f(x - j\Delta x) \right\}$$

Derivation:

Starting with the theory set out on page 19

$$\frac{d^1 f}{dx^1} \equiv \lim_{\Delta x \rightarrow 0} \left\{ \frac{f(x) - f(x - \Delta x)}{\Delta x} \right\}$$

The second derivative is

$$\frac{d^2 f}{dx^2} \equiv \lim_{\Delta x \rightarrow 0} \left\{ \frac{f(x) - 2f(x - \Delta x) + f(x - 2\Delta x)}{[\Delta x]^2} \right\}$$

And the n^{th} derivative can be deduced using the observation that the coefficients are binomial coefficients of alternating sign. Hence

$$\frac{d^n f}{dx^n} \equiv \lim_{\Delta x \rightarrow 0} \left\{ [\Delta x]^{-n} \sum_{j=0}^n [-1]^j \binom{n}{j} f(x - j\Delta x) \right\}$$

In order to define the derivative in terms of a restricted limit and restrict the derivative to discrete values only, a redefinition of dx is needed. The redefinition that allows this is

$$\Delta x = \frac{x - a}{N}$$

Where $N = 1, 2, 3, \dots$ and $a < x$ and is similar to a lower limit in an integral sense. The n th derivative can now be written as

$$\frac{d^n f}{dx^n} \equiv \lim_{\Delta x \rightarrow 0} \left\{ \frac{\sum_{j=0}^{N-1} [-1]^j \binom{n}{j} f(x - j\Delta x)}{[\Delta x]^n} \right\} = \lim_{N \rightarrow \infty} \left\{ \frac{\sum_{j=0}^{N-1} [-1]^j \binom{n}{j} f\left(x - j \left[\frac{x-a}{N}\right]\right)}{\left[\frac{x-a}{N}\right]^n} \right\}$$

Now let $n \equiv g(f, x, t) = g$

$$\frac{d^g f}{dx^g} \equiv \lim_{\Delta x \rightarrow 0} \left\{ \frac{\sum_{j=0}^{N-1} [-1]^j \binom{g}{j} f(x - j\Delta x)}{[\Delta x]^g} \right\} = \lim_{N \rightarrow \infty} \left\{ \frac{\sum_{j=0}^{N-1} [-1]^j \binom{g}{j} f\left(x - j \left[\frac{x-a}{N}\right]\right)}{\left[\frac{x-a}{N}\right]^g} \right\}$$

Using the Gamma definition of $\binom{g}{j}$ gives:

$$\frac{d^g f}{dx^g} \equiv \lim_{\Delta x \rightarrow 0} (\Delta x)^{-g} \left\{ \sum_{j=0}^{N-1} \frac{\Gamma(j-g)}{\Gamma(-g)\Gamma(j+1)} f(x - j\Delta x) \right\}$$

The FOD adds an extra degree of freedom to the standard and fractional derivatives. The function $f(x)$ may well be a function of $F(x)$, in which case the computation of the FOD is akin to solving two simultaneous equations.

The intended application of the FOD is to construct a functional order diffusion equation that will emulate nonlinear mean square deviations w.r.t time.

$$\frac{\partial U}{\partial t} = D(x) \frac{\partial^{\alpha(U, x, t)} U}{\partial x^{\alpha(U, x, t)}} + q(x, t) \quad (46)$$

The functional order diffusion equation is superior to the fractional diffusion equation when applied to the transport behavior of micro-spheres in cells, as in fig 5. The behavior of the mean square deviation is linear at small times, becomes nonlinear at intermediate times and plateaus at long times. The standard fractional diffusion equation only allows for the linear MSD behavior which breaks down at time become large, whereas the functional order diffusion equation has the ability to describe the MSD for all time.

One of the drawbacks of the added functionality of functional order diffusion is that the iteration matrix, A(Eqn 16), depending on the function, may need to be updated at every time step.

Another application of functional order derivatives is that of turbulence and hydrodynamics. The order of fractional diffusion has the ability to define laminar and turbulent behavior in separate spatial and time regions. An interesting concept that could be employed to simulate hydrodynamic flow is that the order could be a function of the Reynolds number.

The Reynolds number[37] is the ratio of inertial forces to viscous forces which is defined as[32]

$$R_e = \frac{\bar{u}d}{\nu} \quad (47)$$

Where \bar{u} is the mean velocity, d is the characteristic length and ν is the kinematic fluid viscosity.

When viscosity is high(i.e.low Reynolds number) the flow is Laminar, which is characterised by smooth flow and fairly constant fluid velocity. The high viscosity prevents mixing, therefore it can be compare with sub diffusion.

When viscosity is low(i.e. high Reynolds number) the flow is turbulent, the inertial forces take charge and the flow is characterised by eddy currents and vortices. These energetic flow patterns increase mixing in the fluid and can be compared to superdiffusion.

Algorithm to Solve the 1D Functional Order Diffusion Equation.

The following simple algorithm describes the procedure for solving the functional order fractional diffusion(FOFD) equation.

$$\frac{\partial u(x,t)}{\partial t} = d(u,x,t) \frac{\partial^\alpha u}{\partial x^\alpha} + q(u,x,t) \quad \alpha \equiv f(u,x,t) \quad (48)$$

The method used is a Crank-Nicholson type finite difference that is an extension of the method described in Tadjeran et al[1].

To reduce computational expense in scheme[1] the Grunwald weights for each value of k (eqn)are pre-calculated and are stored in an array. This pre-calculation of weights cannot be done with FOFD as α is no longer a single value and is in fact a continuum of values. As such, the only way to reduce the computational expense in this case is to only allow for a discretized set of α . The Grunwald weights will now be stored in a 2D array. If non-discretized values of α are to be used then the Grunwald weights must be calculated for each grid point, and in relation to other grid points(if spatially dependant) and at every time step(if time dependant). The method used in the example is the computationally expensive, non-discretized method,

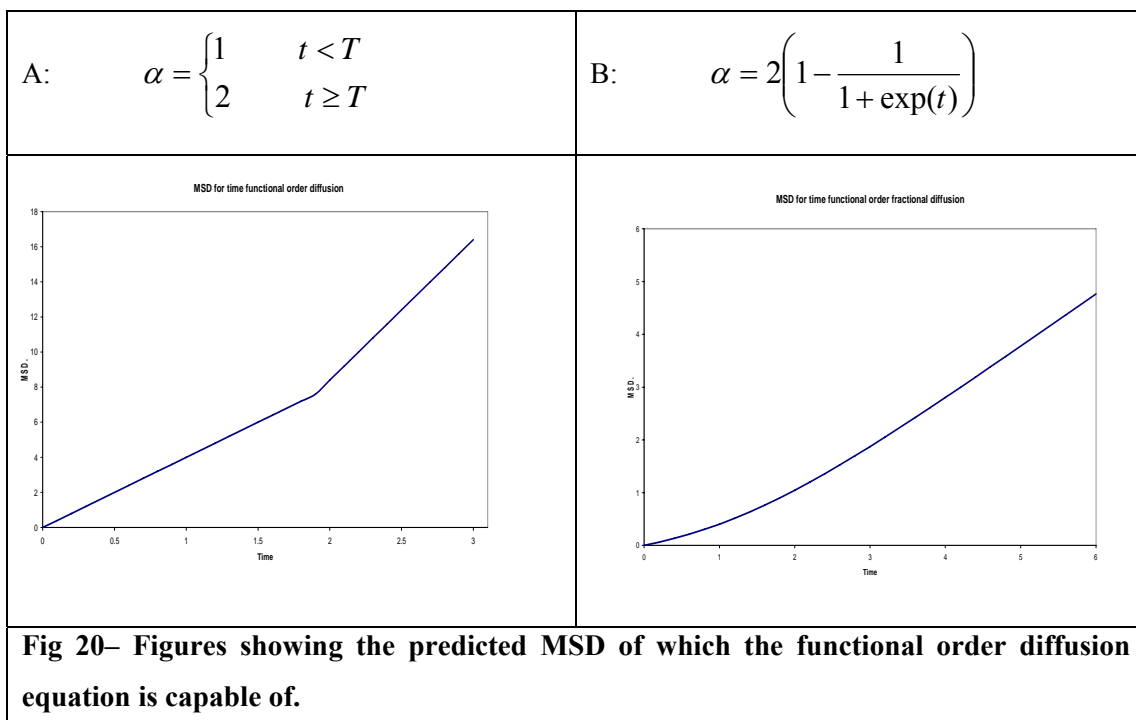
which requires the least modification of the standard 1D example, which is to call the Grunwald weight setting procedure at the same level as the setting of η_i (using the same definitions as in equation 16)(Refer to code in appendix for details). The Richardson extrapolation as used in Tadjeran et al. can also be implemented in order to create a second order accurate method.

In the following pages, the description and theoretical behaviour of two FOFD examples will be presented, both of which, as far as the author is aware is original. Unfortunately, the computational results have not been produced due to time constraints, although predicted/expected solutions will be presented.

FOFD- Time Dependant

Many of the examples of fractional dynamics mentioned in the introduction have a linear MSD(w.r.t time) for a section of the graph but are non linear in other parts. The standard fractional diffusion equation cannot deal with nonlinear time dependant alpha. The functional order diffusion equation has the ability to do this providing the correct function is used to define the evolution of alpha with time.

A step function would have the ability to produce a MSD with two different linear portions(fig 20.A). An sgn(t) could be used to make a more realistic merging effect between linear and nonlinear portions of the MSD(fig 20.B).



FOFD- Spatial Dependence

In the majority of real life examples of fluid dynamics the Reynolds number is spatially dependant. One simple example that could be used to model this principle is the diffusion of a contaminant in a 2D lake of which a portion of the lake has a smooth sand bed and the other portion has a rough rock bed. The sand and rocks would cause laminar(low Reynolds number) and turbulent flow (high Reynolds number) respectively.

The results would look similar to the $\alpha = 1$ plume diffusion on the sand bed and $\alpha=2$ plume diffusion on the rock bed.

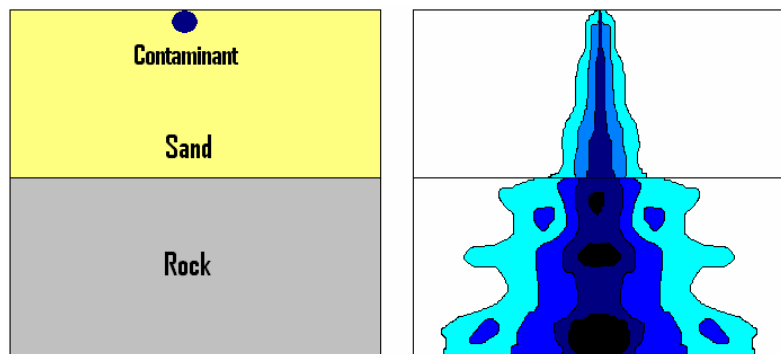


Fig 21 – The expected solution for spatially functional order fractional diffusion.

6 Summary

The subject of fractional dynamics has been studied extensively in the last ten years both empirically and theoretically. The purpose of this report was to summarize some of the key concepts with fractional dynamics (but focusing on fractional diffusion), make a brief account of some its applications and reproduce a few results from influential papers.

The introduction sets out the foundations of diffusion, the measures of it and the methods used to simulate it computationally. The derivation of both the standard and the fractional diffusion equation is then provided along with their solutions. The underlying physics and the link between random walks and diffusion are then discussed and a summary of paper which is illustrative of these ideas is presented. Some simulations of random walks are presented along with applications of random walks, Levy flights, fractional dynamics and fractional diffusion.

The core elements of the report focus of the spatially fractional diffusion equation. The theory of fractional calculus and its application to diffusion is report and then juxtaposed with a 1D simulation of the spatially fractional diffusion equation which is compared to results from Tadjeran et al[1]. This example is based on comparing a computed solution to an exact solution. The order of accuracy for the scheme was found to be the same as Tadjeran et al, however, an extrapolation method which was reported in Tadjeran to increase the order of accuracy to 2nd order was proved Tadjeran analysis to be incorrect. For large step sizes their analysis is correct but as the step size decreases, so does the order of accuracy.

The key breakthrough (for the author at least) is that the spatially fractional, nonsymmetric diffusion equation produces subdiffusion for $1 \leq \alpha < 2$ and **not** superdiffusion as originally expected. The subdiffusion for $1 \leq \alpha < 2$ was then proved theoretically(page 26) using the expectation value operator. $\alpha=1$ is just the advection equation, hence the MSD will not change as the solution of the equation is only shifted right or left, depending on what side operator is used, resulting in no diffusion. $\alpha=0$ results in zero MSD as the solution proportionally shrinks in size with time. As expected, $\alpha=2$ produces standard diffusion which has a linear MSD correlation with time.

Figure 11 proves the theory drawn out on page 24, that $FWHM \propto t^{\alpha/2}$, to be correct. Theoretical results for MSD and FWHM for the symmetric diffusion is difficult and is not provided in this report for two reasons. The first being that the FWHM and MSD relations have not been published for the spatially fractional diffusion equation and the second being time restraints have prevented the research needed to make these calculations.

One of the key concepts of fractional diffusion (and fractional dynamics in general) is that the solution is very different for the symmetric and non-symmetric differential operators. The iteration matrices illustrated on pages 29 and 30 show that for $\alpha=1$ the matrix is equal to the minus of $\alpha=2$.

The results of the MSD show linear behavior of MSD for $\alpha=2$, as expected. The MSD results show a slight subdiffusion for $1<\alpha<2$. The $\alpha=1$ scenario produces a nonlinear correlation with time.

Later in the report solutions to the fractional Fokker-Planck equation with various potentials were created. Both superharmonic and quartic potentials matched the original results presented in Mezler et al.

In the later stages of the report the 2D fractional diffusion equation is computed. A method and test case from Tadjeran et al was implemented. The author's results matched that of Tadjeran et al. Note that the extrapolation method used in the 1D case is not reported for the 2D case as it breaks down for low step sizes, therefore the author decided that the implementation would be of no benefit.

The right sided 2D model was then put aside to focus on the symmetric fractional diffusion equation. Several Gaussian functions were diffused for $\alpha =1.0$, $\alpha =1.5$ and $\alpha =2.0$. The principle of skewness was also demonstrated.

The phenomenon of anomalous plume diffusion was then simulated using the 2D fractional diffusion code with a modification that allows advection. The results show that standard diffusion occurs for integer α and subdiffusion occurs for $1<\alpha<2$.

Finally, an interesting concept, that as far as the author is aware, has yet to be explored is functional order derivatives(FOD's). The derivation of the FOD was presented and applications of FOD's were discussed and testable scenarios were also presented. Unfortunately, time restraints prevented the testable scenarios to be computed.

The subject of fractional dynamics has many avenues that have yet to be researched despite the fact that there is already a vast amount of work already published on the subject. Further work of interest includes:

- The computation of testable scenarios of FOD's.
- A piece future work that was intended for this project is the study of the average behaviour of Levy flights. This would include making several thousand Levy flights for each value of alpha analysing their group behaviour. Theory suggests that Levy flights and fractional diffusion are equivalent and so the future work mentioned will test the theory.
- The modification of fractional diffusion and random walk processes to include particle interaction. This can either be of the form of chemical reactions or annihilations, which would cause the diffusion equation to break down as the continuity equation would need to be modified to include energy and mass.

- Recently, a large amount of work has been published on the subject of relativistic diffusion [40,41]. Creating a fractional relativistic diffusion equation or researching whether FOD can create relativistic diffusion would be an interesting line of inquiry.

La Fin

References

- [1] Charles Tadjeran and Mark M. Meerschaert A second-order accurate numerical method for the two-dimensional fractional diffusion equation. *Journal of Computational Physics*, Volume 220, Issue 2, 10 January 2007, Pages 813-823
- [2] Keith B. Oldham, Jerome Spanier. *The Fractional Calculus*, Dover, New York, 2002. Page 1.
- [3] D.F. Escande, F. Sattin. When can Fokker-Planck Equation describe anomalous or chaotic transport? physics.plasm-ph. May 25th 2007. arXiv:0705.3737v1
- [4] A.M. Lacasta, J.M. Sancho, A.H. Romero, I.M. Sokolov and K.Lindenburg. From subdiffusion to superdiffusion of particles on solid surfaces. *Physical Review E* 70, 051104 (2004).
- [5] <http://en.wikipedia.org/wiki/Nucleotide>. Accessed 04/07/2007.
- [6] P. Allegrini, M. Barbi, P. Grigolini and B.J. West. Fractional diffusion and Lévy stable processes. *Phys.Rev. E* 52, 5281 (1995).
- [7] arXiv:cond-mat/0105041v1 [cond-mat.stat-mech].
- [8] arXiv:physics/0603086 v1 10 Mar 2006
- [9] Mark M. Meerschaert , Charles Tadjeran, Finite difference approximations for fractional advection-dispersion flow equations, *Journal of Computational and Applied Mathematics*, v.172 n.1, p.65-77, 1 November 2004 [doi>10.1016/j.cam.2004.01.033]
- [10] R. Metzler, J. Klafter, The restaurant at the end of the random walk: recent developments in the description of anomalous transport by fractional dynamics, *J. Phys. A* 37 (2004) R161-R208.
- [11] Charles Tadjeran , Mark M. Meerschaert, A second-order accurate numerical method for the two-dimensional fractional diffusion equation, *Journal of Computational Physics*, v.220 n.2, p.813-823, January, 2007
- [12] Ralf Mezler, Aleksei V. Chechkin, Joseph Klafter. Levy statistics and anomalous transport: Levy flights and subdiffusion. arXiv:0706.3553v1[cond-mat.stat-mech] 25 June 2007.
- [13] http://en.wikipedia.org/wiki/Fokker-Planck_equation. Accessed 05/06/2007
- [14] Keith B. Oldham, Jerome Spanier. *The Fractional Calculus*, Dover, New York, 2002. Page 26.
- [15] Keith B. Oldham, Jerome Spanier. *The Fractional Calculus*, Dover, New York, 2002. Page 28.
- [16] K. Miller, B. Ross, *An Introduction to the Fractional Calculus and Fractional Differential*, Wiley. New York, 1993.

- [17] Guy Jumarie. Merton's model of optimal portfolio in a Black-Scholes Market driven by a fractional Brownian motion with short-range dependence. *Insurance: Mathematics and Economics*, Volume 37, Issue 3, 16 December 2005, Pages 585-598
- [18] Fredrick Michael and M. D. Johnson, *Physica A: Statistical Mechanics and its Applications* Volume 324, Issues 1-2, 1 June 2003, Pages 359-365
- [19] [http://en.wikipedia.org/wiki/Robert_Brown_\(botanist\)](http://en.wikipedia.org/wiki/Robert_Brown_(botanist))
- [20] A. Einstein, *Ann. Phys. (Leipzig)* 17, 549 (1905)
- [21] R. Brown, *Edin. New Phil.* 5, 358 (1828)
- [22] Keith B. Oldham, Jerome Spanier. *The Fractional Calculus*, Dover, New York, 2002. Page 14.
- [23] Viviane M. de Oliveira, M.A.F. Gomes, I.R. Tsang. *Physica A: Statistical Mechanics and its Applications* Volume 361, Issue 1, 15 February 2006, Pages 361-370
- [24] Caspi A, Granek R and Elbaum M. 2002 *Phys. Rev. E* 66 011916
- [25] Stanislav Boldyrev, Carl R. Gwinn. Lévy Model for Interstellar Scintillations *Phys. Rev. Lett.* 91, 131101 (2003)
- [26] D. S. Novikov, M. Drndic, L. S. Levitov, M. A. Kastner, M. V. Jarosz, M. G. Bawendi. Levy statistics and anomalous transport in quantum-dot arrays. *Phys. Rev. B* 72, 075309 (2005)
- [27] Emmanuel Hanert. On the use of stable distributions to represent turbulent mixing. August 2006
- [28] N. Laskin. Fractional Schrodinger equation. *Quantum Physics (quant-ph)*. June 2002
- [29] Cascaval R.C.; Eckstein E.C.; Frota C.L.; Goldstein J.A. Fractional telegraph equations. *Journal of Mathematical Analysis and Applications*, Volume 276, Number 1, December 2002, pp. 145-159(15)
- [30] Orsingher, Enzo; Beghin, Luisa. Time-fractional telegraph equations and telegraph processes with brownian time. *Probability Theory and Related Fields*, Volume 128, Number 1, January 2004, pp. 141-160(20)
- [31] Tarasov, Vasily E. Fractional Hydrodynamic Equations for Fractal Media. *Annals of Physics* 318 (2005) 286-307
- [32] <http://scienceworld.wolfram.com/physics/ReynoldsNumber.html>. Accessed 16/08/2007.
- [33] <http://mathworld.wolfram.com/FunctionalDerivative.html> Accessed 16/08/2007.
- [34] http://www.itp.physik.tu-berlin.de/brandes/public_html/publications/notes05/node70.html. Accessed 16/08/2007
- [35] Alexander Dynin. Functional derivatives, Schrödinger equations, and Feynman integration. *Mathematical Physics (math-ph)*. arXiv:math-ph/0703088

- [36] <http://mathworld.wolfram.com/FunctionalDerivative.html>. Accessed 16/08/2007
- [37] Frisch U., Turbulence. The legacy of A.N. Kolmogorov, Cambridge University Press, (1995)
- [38] Marek Gutowski. Levy flights as an underlying mechanism for global optimization algorithms. arXiv:math-ph/0106003 v1 4 jun 2001
- [39] NASA - http://science.nasa.gov/headlines/y2003/29dec_magneticfield.htm
- [40] Kazinski, P. O. Relativistic diffusion equation from stochastic quantization. arXiv:0704.3877
- [41] Debbasch F.; Rivet J.P. ; A Diffusion Equation from the Relativistic Ornstein–Uhlenbeck Process. Journal of Statistical Physics, Volume 90, Numbers 5-6, March 1998 , pp. 1179-1199(21)